



Year: 2021

The JAK inhibitor tofacitinib rescues intestinal barrier defects caused by disrupted epithelial-macrophage interactions

Spalinger, Marianne R ; Sayoc-Becerra, Anica ; Ordookhanian, Christ ; Canale, Vinicius ; Santos, Alina N ; King, Stephanie J ; Krishnan, Moorthy ; Nair, Meera G ; Scharl, Michael ; McCole, Declan F

Abstract: BACKGROUND AND AIMS Loss-of-function variants in protein tyrosine phosphatase non-receptor type-2 (PTPN2) promote susceptibility to inflammatory bowel diseases (IBD). PTPN2 regulates Janus-kinase (JAK) and signal transducer and activator of transcription (STAT) signaling, while protecting the intestinal epithelium from inflammation-induced barrier disruption. The pan-JAK inhibitor, tofacitinib, is approved to treat ulcerative colitis but its effects on intestinal epithelial cell-macrophage interactions and on barrier properties are unknown. We aimed to determine if tofacitinib can rescue disrupted epithelial-macrophage interaction and barrier function upon loss of PTPN2. METHODS Human Caco-2BBE intestinal epithelial cells (IECs) and THP-1 macrophages expressing control or PTPN2-specific shRNA were co-cultured with tofacitinib or vehicle. Transepithelial electrical resistance and 4 kDa fluorescein-dextran flux were measured to assess barrier function. Ptpn2^{fl/fl} and Ptpn2-LysMCre mice, which lack Ptpn2 in myeloid cells, were treated orally with tofacitinib citrate twice daily to assess the in vivo effect on the intestinal epithelial barrier. Colitis was induced via administration of 1.5% DSS in drinking water. RESULTS Tofacitinib corrected compromised barrier function upon PTPN2 loss in macrophages and/or IECs via normalization of (i) tight junction protein expression, (ii) excessive STAT3 signaling, and (iii) IL-6 and IL-22 secretion. In Ptpn2-LysMCre mice, tofacitinib reduced colonic pro-inflammatory macrophages, corrected underlying permeability, and prevented the increased susceptibility to DSS colitis. CONCLUSIONS PTPN2 loss in IECs or macrophages compromises IEC-macrophage interactions and reduces epithelial barrier integrity. Both of these events were corrected by tofacitinib in vitro and in vivo. Tofacitinib may have greater therapeutic efficacy in IBD patients harboring PTPN2 loss-of-function mutations.

DOI: <https://doi.org/10.1093/ecco-jcc/jjaa182>

Posted at the Zurich Open Repository and Archive, University of Zurich

ZORA URL: <https://doi.org/10.5167/uzh-190593>

Journal Article

Accepted Version

Originally published at:

Spalinger, Marianne R; Sayoc-Becerra, Anica; Ordookhanian, Christ; Canale, Vinicius; Santos, Alina N; King, Stephanie J; Krishnan, Moorthy; Nair, Meera G; Scharl, Michael; McCole, Declan F (2021). The JAK inhibitor tofacitinib rescues intestinal barrier defects caused by disrupted epithelial-macrophage interactions. *Journal of Crohn's Colitis*, 15(3):471-484.

DOI: <https://doi.org/10.1093/ecco-jcc/jjaa182>

The JAK inhibitor tofacitinib rescues intestinal barrier defects caused by disrupted epithelial-macrophage interactions.

Marianne R. Spalinger^{1,*}, Anica Sayoc-Becerra^{1,*}, Christ Ordookhanian¹, Vinicius Canale¹, Alina N. Santos¹, Stephanie J. King¹, Moorthy Krishnan¹, Meera G. Nair¹, Michael Scharl², and Declan F. McCole^{1§}

¹Division of Biomedical Sciences, University of California, Riverside, CA.

²Department for Gastroenterology and Hepatology, University Hospital Zurich, Zurich, Switzerland

* These authors contributed equally

§Corresponding author: Declan F. McCole, PhD, Division of Biomedical Sciences, School of Medicine, University of California Riverside, 307 School of Medicine Research Building, 900 University Avenue, Riverside, CA 92521; Tel: (951) 827-7785; E-mail: declan.mccole@ucr.edu

Short title: Tofacitinib corrects intestinal permeability defects

19 **ABSTRACT (max 250 words)**

20 **Background and Aims:** Loss-of-function variants in protein tyrosine phosphatase non-receptor
21 type-2 (*PTPN2*) promote susceptibility to inflammatory bowel diseases (IBD). *PTPN2* regulates
22 Janus-kinase (JAK) and signal transducer and activator of transcription (STAT) signaling, while
23 protecting the intestinal epithelium from inflammation-induced barrier disruption. The pan-JAK
24 inhibitor, tofacitinib, is approved to treat ulcerative colitis but its effects on intestinal epithelial
25 cell–macrophage interactions and on barrier properties are unknown. We aimed to determine if
26 tofacitinib can rescue disrupted epithelial-macrophage interaction and barrier function upon loss
27 of *PTPN2*.

28 **Methods:** Human Caco-2BBE intestinal epithelial cells (IECs) and THP-1 macrophages
29 expressing control or *PTPN2*-specific shRNA were co-cultured with tofacitinib or vehicle.
30 Transepithelial electrical resistance and 4 kDa fluorescein-dextran flux were measured to assess
31 barrier function. *Ptpn2*^{fl/fl} and *Ptpn2*-LysMCre mice, which lack *Ptpn2* in myeloid cells, were
32 treated orally with tofacitinib citrate twice daily to assess the *in vivo* effect on the intestinal
33 epithelial barrier. Colitis was induced via administration of 1.5% DSS in drinking water.

34 **Results:** Tofacitinib corrected compromised barrier function upon *PTPN2* loss in macrophages
35 and/or IECs via normalization of (i) tight junction protein expression, (ii) excessive STAT3
36 signaling, and (iii) IL-6 and IL-22 secretion. In *Ptpn2*-LysMCre mice, tofacitinib reduced
37 colonic pro-inflammatory macrophages, corrected underlying permeability, and prevented the
38 increased susceptibility to DSS colitis.

39 **Conclusions:** *PTPN2* loss in IECs or macrophages compromises IEC-macrophage interactions
40 and reduces epithelial barrier integrity. Both of these events were corrected by tofacitinib *in vitro*

and *in vivo*. Tofacitinib may have greater therapeutic efficacy in IBD patients harboring *PTPN2* loss-of-function mutations.

Key words: TCPTP, IBD, permeability, tight junction, JAK-STAT, epithelial cells, macrophage

Funding

This work was supported by a postdoctoral research stipend from the Swiss National Science Foundation (project number P300PB_177932) to MRS, UC Riverside School of Medicine Medical Student Externship Scholarship to CO, research support from the NIH (R21AI137830) to MGN, research support from the NIH (2R01DK091281, 1R01AI153314) to DFM, an ASPIRE-Pfizer 2017 IBD Research Award (W1227049) to DFM, and a Pfizer Global Medical Grants 2020 Research Award (59444033) to DFM.

Data availability

The data underlying this article are available in the article and in its online supplementary material.

INTRODUCTION

Inflammatory bowel diseases (IBD) are chronic inflammatory conditions of the digestive tract, which manifest as diarrhea, abdominal pain, ulcers, and in severe cases, anemia and micronutrient deficiency. IBD encompasses ulcerative colitis (UC) and Crohn's disease (CD), which differ in their histopathology and the affected intestinal regions.¹⁻³ IBD is multi-factorial, with genetic, environmental, immunological and microbial factors contributing to disease manifestation.⁴ Due to the complex pathogenesis of IBD, most current therapeutic strategies alleviate IBD symptoms, rather than target specific disease-driving molecular pathways.^{5,6} Biologics, such as anti-TNF treatment emerged as an effective treatment for IBD, but 30-50% of patients lose clinical response to anti-TNF treatment,^{7,8} partially due to production of anti-drug antibodies,⁹ thus alternative treatment strategies are being developed and/or tested for use in IBD.

Tofacitinib (Xeljanz®) is a small-molecule pan-Janus kinase (JAK) inhibitor approved for the treatment of moderate-to-severe ulcerative colitis. JAK family molecules are mediators of pro-inflammatory cytokine signaling, and tofacitinib has proven effective in treating chronic diseases, including IBD.¹⁰⁻¹³ However, only 40.6% of UC patients showed sustained clinical remission under tofacitinib treatment thus indicating that only a proportion of patients are responsive.¹² While pre-clinical animal studies have investigated the effects of tofacitinib on models of intestinal inflammation, studies of specific cell types in the gut (i.e. intestinal epithelial cells and macrophages) targeted by tofacitinib are limited in number.¹⁴⁻¹⁶

The barrier function of the intestinal epithelium ensures separation of luminal contents from underlying tissues while allowing regulated passage of fluid and electrolytes. Tight junctions, which consist of several transmembrane proteins, selectively seal the paracellular

space between intestinal epithelial cells (IECs) and control the passage of water and ions.^{17,18} Epithelial barrier disruption allows bacteria and bacterial components to penetrate the epithelium and to initiate immune responses, which in turn have detrimental effects on the tight junction complex.¹⁹ Increased intestinal permeability is an early feature of IBD²⁰ that precedes intestinal inflammation and is a prognostic factor for relapse in Crohn's disease.²¹⁻²⁵ Moreover, a recent prospective study of a large cohort of asymptomatic first-degree relatives of IBD patients identified that increased intestinal permeability is significantly associated with increased future risk of developing Crohn's disease, and thus represents a separate pre-disease risk factor for later onset of Crohn's disease independent of potential subclinical inflammation²⁶.

Over 240 single-nucleotide polymorphisms (SNP) have been associated with increased risk for IBD, including protein tyrosine phosphatase non-receptor type 2 (*PTPN2*), which encodes the T cell protein tyrosine phosphatase (TCPTP).^{4,27-30} IBD-associated single nucleotide polymorphisms (SNPs) within the *PTPN2* gene locus have been reported to result in decreased *PTPN2* expression³¹ and TCPTP phosphatase activity³², while a recent report showed that a loss-of-function mutation in the phosphatase domain encoding region of *PTPN2* results in loss of TCPTP activity and very early onset intestinal inflammation³³. The most studied *PTPN2* variants in the context of IBD are SNP rs1893217 and SNP rs2542151. These two SNPs are in linkage disequilibrium³² and have a minor allele frequency of approximately 16% in the general population and 20% in IBD patients²⁷, although geographic regional differences exist²⁷. Substrates of TCPTP include members of the JAK-signal transducer and activator of transcription (STAT) signaling pathway.³⁴⁻³⁶ Constitutive *Ptpn2*^{-/-} mice exhibit intestinal inflammation and succumb to systemic inflammation between 3-5 weeks of age.³⁷ Knockdown of *PTPN2* in human IEC cultures promotes STAT activation and enhances barrier defects in the

104 presence of the pro-inflammatory cytokine IFN- γ .³⁸ In a model of naïve T cell transfer-mediated
105 colitis, RAG2 knockout mice injected with *Ptpn2*-deficient T cells showed increased STAT1 and
106 STAT3 levels.³⁹ Further, *Ptpn2*-LysMCre mice, which lack TCPTP primarily in macrophages
107 and monocytes, are more susceptible to acute DSS-induced colitis.⁴⁰ Recently, we have shown
108 that TCPTP loss in macrophages affects IEC properties (i.e. barrier function), and in turn,
109 TCPTP-deficient IECs alter macrophage functions and cytokine secretion⁴¹. Further, JAK-
110 inhibition by tofacitinib reduced IFN- γ -induced barrier dysfunction in IEC lines and human
111 colon organoids through modulation of tight junction molecules.⁴² Here, we translate earlier
112 findings in individual cell types to relevant co-culture and *in vivo* models to show that tofacitinib
113 directly affects IEC and macrophage cell function. Moreover, tofacitinib also corrects defects in
114 the interactions between these cell types, culminating in increased intestinal permeability, that
115 arise from TCPTP deficiency and elevated JAK-STAT signaling.

MATERIALS AND METHODS

Cell culture

Human Caco-2BBE intestinal epithelial cells (IECs) were cultured in Dulbecco's Modification of Eagle's Medium (DMEM, #15-017-CV, Corning, Corning, NY) supplemented with 10% heat-inactivated fetal bovine serum (Thermo Fisher Scientific, Waltham, MA) and 1% L-glutamine (Lonza, 17-605E, Walkersville, MD). Human THP-1 cells were cultured in RPMI 1640 medium (#10-040-CV, Thermo Fisher Scientific) with 10% heat-inactivated fetal bovine serum (Thermo Fisher Scientific). All cells were grown in standard 12-well cell culture plates (#130185, ThermoScientific, Rochester, NY) or transwell membranes (#3460, Corning, Kennebunk, ME) in a humidified incubator at 37°C with 5% CO₂.

Generating stable shRNA PTPN2-deficient cell lines

Cell lines stably expressing *PTPN2* shRNA were generated as previously described.^{43,44} Briefly, Caco-2BBE and THP-1 cells were infected with lentiviral constructs containing either *PTPN2*-specific, or non-targeting scrambled shRNA. After 72 h of infection, stable cell lines were selected using puromycin (400-128P, Gemini, New York, NY). Stable Caco-2BBE and THP-1 control (Ctr) and *PTPN2* knockdown (KD) cell lines were maintained at 4 µg/mL and 0.5 µg/mL puromycin, respectively. Knockdown of *PTPN2*/TCPTP was confirmed by qPCR and Western blotting⁴¹.

Measurement of transepithelial electrical resistance and 4 kDa FITC-dextran permeability in vitro

Transepithelial electrical resistance (TEER) of Caco-2BBe cells grown on transwells was measured using an EVOM2 Epithelial Voltohmmeter (World Precision Instruments, Sarasota, FL). Values from an empty well were subtracted, and readings multiplied by the transwell surface area and expressed as Ohms•cm². After measurement of TEER, cells were washed twice and equilibrated in 1X PBS with CaCl₂ and MgCl₂ (D8662, Sigma-Aldrich, St. Louis, MO) for 30 min at 37°C. Fluorescein isothiocyanate (FITC)-4 kDa dextran (FD4, 1mg/ml, Sigma-Aldrich) was added to the apical side, and after 2 h at 37°C, fluorescence of duplicate samples from the basolateral medium was measured using a microplate reader (Promega, Madison, WI). FD4 concentrations were calculated against a standard curve.

Co-culture experiments and tofacitinib treatments in vitro

Caco-2BBe IECs were seeded on transwell membranes at 0.5×10^6 cells per well and cultured for 8 days. Cells were then switched to serum-free media overnight before co-culture with THP-1 cells and/or treated with tofacitinib. Prior to co-cultures with IECs, 0.25×10^6 THP-1 monocytes were pulsed for 3 h with PMA (Sigma-Aldrich) to induce macrophage differentiation, seeded on 12-well standard cell culture plates for 48 h, and then switched to serum-free DMEM the day before the experiment. Prior to start of the co-culture, Caco-2BBe cells were pre-treated apically with vehicle (dimethyl sulfoxide, DMSO, 0.5%, Sigma-Aldrich) or tofacitinib (50 μ M, MedChemExpress, Monmouth Junction, NJ) for 1 h followed by placing the transwells into the THP-1 cell-containing 12-well plates. After 24 h, TEER and FD4 permeability were measured, the basolateral media collected, and protein from both Caco-2BBe and THP-1 cells harvested.

Harvesting and preparation of whole cell protein lysates

For protein isolation, cells were washed twice with ice-cold 1X PBS with CaCl_2 and MgCl_2 (D8662, Sigma-Aldrich) prior to lysis with RIPA lysis buffer (50 mM Tris-Cl pH 7.4, 150 mM NaCl, 1% NP-40, 0.5% sodium deoxycholate, and 0.1% SDS) supplemented with 1X protease inhibitor (Roche, South San Francisco, CA), 2mM sodium fluoride, 2mM PMSF, and phosphatase inhibitors (2mM sodium orthovanadate, 1X Phosphatase Inhibitor Cocktail 2 and 3, Sigma-Aldrich) for 15 min at 4°C. Cells were scraped, transferred into microcentrifuge tubes and homogenized on ice using the Q125 Sonicator (QSonica Sonicators, Newtown, CT). Cell lysates were centrifuged at 16, 200 x g at 4°C for 10 min and the supernatants collected into new microcentrifuge tubes. Loading samples were prepared by mixing the same amount of total protein from each sample with Laemmli loading buffer (60 mM Tris-Cl pH 6.8, 2% SDS, 5% β -mercaptoethanol, 0.01% bromophenol blue, and 10% glycerol), and boiling at 95°C for 10 min.

Western blot

Proteins were separated by SDS-polyacrylamide gel electrophoresis, followed by transfer onto polyvinylidene difluoride membranes (EMD Millipore, Temecula, CA). Membranes were blocked with 3% milk, 1% BSA in TBS-T (Tris-buffered saline with 0.1% Tween-20) for 1 h at room temperature, followed by overnight incubation with primary antibodies (see Supplementary Table 1) at 4°C overnight. The following day, membranes were rinsed with TBS-T (x3) then subjected to 5 min washes (x3) with TBS-T and then incubated with horseradish peroxidase-conjugated goat anti-mouse or goat anti-rabbit IgG secondary antibodies (Supplementary Table 1) in 3% milk, 1% BSA in TBS-T for 1 h at room temperature, and again washed with TBS-T (x3). Finally, membranes were incubated with SuperSignalTM West Pico PLUS

Chemiluminescent Substrate solution (Thermo Fisher Scientific) and immunoreactive proteins were detected by exposing the membranes to X-ray film (LabScientific Inc., Highlands, NJ). Densitometric analysis of the blots was performed using ImageJ software.⁴⁵

Immunofluorescence staining

Caco-2 cells were grown on cover slides and cultured for 24 h with conditioned medium from macrophages as previously described⁴¹. Cells were washed 3 x in PBS, fixed in 100% methanol (20 min at -20°C), washed 3 x in PBS, permeabilized with Triton X (1% Triton X-100 in PBS) for 30 min, washed 3 x in PBS containing 0.1% Tween (PBST), and incubated with 10% normal donkey serum in PBST for 1 h prior to incubation with anti ZO-1 antibody (1:200, Thermo Fisher Scientific) overnight at 4°C. Slides were washed three times with PBST, incubated with secondary antibody (anti-Rabbit AlexaFluor 488, 1:200, Jackson ImmunoResearch) for 1 h at room temperature, washed 3 x in PBST, and mounted using ProlongGold Antifade Reagent with DAPI (Thermo Fisher Scientific).

For *in vivo* evaluation of tight junction molecules, OCT-embedded frozen sections were cut into 5 µm sections, slides brought to room temperature, rinsed 2 times with PBST, and fixed in methanol (10 min at -20°C). Slides were incubated in blocking buffer (PBS + 2% donkey serum, 1% BSA, 1% Triton X, 0.05% Tween-20) for 1 h prior to overnight incubation with F'ab donkey-anti-mouse antibody (Jackson ImmunoSearch Inc, West Grove, PA). The slides were rinsed with PBST, incubated with mouse-anti-claudin-2, rabbit anti-ZO-1 and goat anti-E-cadherin antibody (all from Thermo Fisher Scientific, diluted in PBS + 5% normal donkey serum) for 30 minutes at room temperature, rinsed again with PBS prior to incubation with a biotinylated secondary anti-mouse antibody (Jackson ImmunoSearch Inc.) for 20 minutes

followed by an additional wash in PBST, and subsequent incubation with Alexa Fluor 488-steptavidin, Alexa Fluor 647-anti-rabbit secondary antibody and Cy3-anti-goat secondary antibody (Jackson ImmunoSearch) for 30 minutes and finally mounted with ProlongGold Antifade Reagent with DAPI (Thermo Fisher Scientific).

Mice

C57Bl/6 male and female mice homozygous for a floxed *Ptpn2* gene and heterozygous for the LysMCre construct (*Ptpn2*-LysMCre mice, originally generated at the University Hospital Zurich, Zurich, Switzerland) and their LysMCre negative littermates (*Ptpn2*^{fl/fl} mice) were used for all studies.^{40,46} All animal experiments were conducted with approval from the Institutional Animal Care and Use Committee at the University of California, Riverside in accordance with the National Institute of Health guidelines for the use of live animals. 8-14 week old male and female mice housed in a specific pathogen-free (SPF) facility under a 12-h light/dark cycle and food/water *ad libitum* were used for all studies.

Tofacitinib citrate treatment in vivo

Vehicle solution was prepared by dissolving methylcellulose (M7027, Sigma-Aldrich) at 1% w/v in PBS. Tofacitinib citrate gavage solution was prepared fresh every day by resuspending tofacitinib citrate powder (Selleckchem, Houston, TX) in vehicle solution. Gavage solutions were sonicated using the Q125 Sonicator (QSonica Sonicators) at 30% amplitude for 2 min at 10 sec ON/OFF intervals at room temperature. Mice were orally gavaged with vehicle (5 µL per g body weight) or tofacitinib citrate (50mg/kg body weight, in 5 µL per g body weight, concentration based on a previous study¹⁴) twice daily for 7 days (barrier measurements without

colitis induction) or 10 days (experiments with colitis induction). The amount of gavage solution was adjusted on a daily basis according to the weight of each individual and ranged from 80-120 μ L.

Measurement of intestinal permeability in vivo

To assess barrier permeability *in vivo*, mice were food-deprived for 2 h prior to oral administration (200 μ L) of gavage solution containing 100 mg/mL creatinine (#4255, Sigma-Aldrich), 80 mg/mL FD4 (#46944, Sigma-Aldrich) and 20 mg/mL Rhodamine B-dextran 70kDa (RD70, #R9379, Sigma-Aldrich) dissolved in MilliQ H₂O and filtered through a 0.2 μ M syringe filter. A water-gavaged mouse was used as control. After 5 h, blood samples were collected and serum concentrations of the three probes determined as previously described^{41,47}. At this point, animals were given access to food.

Colitis induction

12-14 week old *Ptpn2*-LysMCre mice and their *Ptpn2*^{fl/fl} littermates were treated with tofacitinib citrate as described above for 10 days, starting three days prior to DSS exposure for 7 days (1.5% in the drinking water; MP Biomedicals, Irvine, CA). Body weight and disease scores (based on activity level, stool consistency, weight loss, blood in stool scores) were recorded daily. At day 7 of DSS administration, the mice were euthanized, colon length measured, and the most distal 2 cm of the colon collected for histological assessment of colitis severity as described previously.⁴⁸ The most distal section of the colon was used in order to assess the beneficial effect of tofacitinib on the intestinal region that is most affected by inflammation in the DSS model.

Tissue collection

Intestinal tissues were snap-frozen in liquid nitrogen for protein expression and ELISA analyses. To isolate IECs, proximal colons were everted and incubated in Cell Recovery Solution (#354253, Corning) on ice for 2 h then vigorously shaken to release IECs. IECs were washed twice with ice-cold PBS and proteins isolated as described above.

Flow cytometry

After removal of IECs, intestinal tissues were cut into 0.5 cm pieces and digested with Collagenase type IV (0.6 mg/ml; Sigma-Aldrich, #C5138) for 15 min. Digested tissue pieces were then passed three times through a 18.5 G needle and homogenates filtered through a 7 μ m cell strainer (BD Biosciences; Franklin Lakes, NJ). Cells were washed once with PBS before resuspension in 20 μ L PBS containing Fc-receptor blocking antibodies for 10 min, before adding 20 μ L of fluorescence-labeled antibodies (see Supplementary Table 2) and incubation on ice for 30 min. Samples were washed twice with ice-cold PBS, resuspended in 200 μ L FACS buffer (PBS, 2% FBS) and acquired on an LSR-II flow cytometer from BD Biosciences.

RNA isolation, RT-PCR, and quantitative PCR

Total RNA was isolated from whole proximal colons using RNeasy Mini Kit (Qiagen) per manufacturer's directions. RNA concentration was measured by absorbance at 260 nm and 280 nm using Nanodrop 2000c (Thermo Scientific, Rockford, IL) and reverse transcribed into complementary DNA (cDNA) using qScript cDNA SuperMix (Quantabio, Beverly, MA). qPCR was performed using iQ SYBR Green Supermix (Bio-Rad, Hercules, CA) and an IQ5 Real-Time PCR Thermal Cycler (Bio-Rad). Primers used for murine *Il6*, *Il10*, *Il22*, and *Gapdh* are listed in

Supplementary Table 3. Gene expression was calculated using the average C_T values of triplicate readings normalized to the average of housekeeping gene *Gapdh* C_T values. *Gapdh* was chosen as the housekeeping gene based on a previous evaluation of several housekeeping genes, where *Gapdh* was found most stable in our experimental settings (data not shown). Results were analyzed using the $\Delta\Delta C_T$ method.

Statistical Analysis

Data are presented as mean \pm SD for n number of biological replicates. Animal data are presented as mean \pm SD for one of two independent experiments, each with four to six mice as indicated in the figure legends. Statistical analysis was performed using ANOVA followed by Tukey's or Holm-Sidak post-test. P values of ≤ 0.05 were considered significant.

RESULTS

Tofacitinib corrects elevated permeability in IECs lacking PTPN2 and abrogates the effects of PTPN2-deficient macrophages on barrier function

To determine how macrophages influence IEC barrier function, and whether tofacitinib influences this cross-regulation, THP-1 cells were co-cultured with polarized Caco-2BBe cells that were treated with either vehicle or tofacitinib. As we have recently shown⁴¹, co-culture with control (Ctr) THP-1 macrophages tightened the epithelial barrier with increased TEER and reduced FD4 permeability, while co-culture with *PTPN2* KD THP-1 cells resulted in a leaky barrier, i.e. reduced TEER and increased FD4 flux (Figure 1A+B). Treatment with tofacitinib for 24 h, prevented both of these effects (Figure 1). As previously shown,^{43,44} TEER was significantly lower in resting *PTPN2*-deficient IECs compared to control IECs and co-culture with macrophages did not promote barrier tightness (i.e. no induction of TEER or reduced FD4 flux), while co-culture with *PTPN2* KD THP-1 further decreased TEER and increased FD4 permeability in *PTPN2*-deficient IECs (Figure 1 and ref. ⁴¹). Of note, tofacitinib treatment completely abrogated these effects (Figure 1). Moreover, tofacitinib rescued the TEER of *PTPN2*-deficient Caco-2BBe cells to levels comparable to those of control Caco-2BBe cells (Figure 1A). These results show that the presence of control THP-1 macrophages induces tightening of the epithelial barrier while *PTPN2*-deficient macrophages promote paracellular passage of ions and macromolecules. Both of these effects on the IEC monolayer were abrogated by tofacitinib. These results demonstrate that JAK inhibition is sufficient to rescue the barrier defects observed in *PTPN2*-deficient IECs alone, or in IECs cultured in the presence of *PTPN2*-deficient macrophages.

Tofacitinib prevents macrophage-induced changes in the expression of tight junction proteins

While the paracellular flux of macromolecules is mainly dictated by the presence and/or localization of tight junction proteins (e.g. occludin, tricellulin, JAM-A and ZO-1) the major influence on TEER, which fluctuates due to paracellular passage of ions, is mediated by changes in the charge- and size-selective family of claudin proteins.^{49,50} Consistent with previous findings⁴¹, and with the reduced TEER and increased macromolecular passage upon loss of TCPTP in macrophages and/or IECs, we observed increased expression of the pore-forming molecule claudin-2 and decreased expression of the barrier-sealing proteins junctional adhesion molecule (JAM-A), occludin, tricellulin, and claudin-4 in those cells. Consistent with the normalization of TEER, tofacitinib treatment normalized claudin-2 expression in co-culture groups and partly restored expression of claudin-4 in *PTPN2* KD Caco2-BBe cells, though these still remained lower than control Caco2-BBe cells (Figure 2A, 2B, 2C). In addition, we observed molecule-specific changes in the expression of barrier-sealing proteins: while occludin and JAM-A were both reduced in *PTPN2*-deficient IECs and in Ctr IECs co-cultured with *PTPN2*-deficient macrophages, JAM-A but not occludin was further decreased upon loss of *PTPN2* in both cell types. Notably, only the suppressive effect on occludin was rescued by tofacitinib, while tofacitinib treatment was not able to restore JAM-A levels. In contrast, tricellulin levels were only reduced when *PTPN2* was absent in macrophages, and this effect was only rescued by tofacitinib treatment in Ctr IECs and not in *PTPN2*-deficient IECs (Figure 2A, 2D, 2F). Of note, while tofacitinib was able to normalize the expression of claudin-2 and occludin (Figure 2A, 2E), it also suppressed the induction of tricellulin and JAM-A observed upon co-culture with Ctr macrophages (Figure 2A, 2D, 2F). In addition to these changes in the expression of tight junction molecules, co-culture of Caco-2BBe cells with KD macrophages, or deletion of *PTPN2* in Caco-

2BBe cells also promoted internalization of the tight junction molecule ZO-1 and gap formation between neighboring IECs, effects completely normalized upon treatment with tofacitinib. TCPTP protein expression in IECs remained unchanged by co-culture with macrophages, tofacitinib treatment, or in combination (Figure 2A, 2G). Collectively, these results suggest that changes in the expression patterns of tight junction proteins are individual and distinct and that tofacitinib rescues the underlying barrier defect of *PTPN2*-deficient IECs, at least in part, through effects on claudin-2, claudin-4 and occludin.

Elevated STAT1 and STAT3 phosphorylation in PTPN2-deficient IECs or macrophages are normalized by tofacitinib

TCPTP, the protein product of *PTPN2*, dephosphorylates several members of the JAK-STAT signaling pathway, including JAK1 and JAK3 that are targeted by tofacitinib. Caco-2BBe cells lacking *PTPN2* had significantly higher STAT1 and STAT3 phosphorylation (Figure 3A+B), which were both effectively reduced upon treatment with tofacitinib for 24 h. These data show that tofacitinib can correct the elevated JAK-STAT activation in IECs with *PTPN2* loss. Furthermore, co-culture with macrophages significantly increased STAT1 and STAT3 phosphorylation in control Caco-2BBe, both of which were normalized upon tofacitinib treatment (Figure 3A+B).

Similarly, and consistent with findings among other *PTPN2*-deficient models, macrophages lacking *PTPN2* had elevated JAK1 and STAT1 phosphorylation, which was further enhanced upon co-culture with either control or *PTPN2*-KD IECs, and again fully reversed by tofacitinib (Figure 4A+B). Co-culture of control THP-1 cells with *PTPN2*-deficient Caco-2BBe cells also induced JAK1 and STAT1 phosphorylation, and this was completely negated by

tofacitinib treatment (Figure 4A+B). STAT3 phosphorylation levels followed the same pattern in *PTPN2*-deficient macrophages, but in general, levels of phosphorylated STAT3 were rather low (Figure 4C). These results demonstrate that in control macrophages, JAK1 is activated in the presence of *PTPN2*-deficient IECs, but not in the presence of IECs that express normal *PTPN2* levels. However, co-culture with IECs of either genotype induced JAK1 and STAT1 phosphorylation in both control and *PTPN2*-deficient THP-1 cells, though to a much larger extent in *PTPN2* KD THP-1 cells, perhaps due to the elevated basal JAK1/STAT1 phosphorylation. Overall, tofacitinib inhibited JAK-STAT signaling in macrophages co-cultured with IECs and reduced the significantly elevated level of JAK-STAT activation in *PTPN2* KD macrophages to background levels.

IL-6, IL-22, and TNF- α secretion is induced by *PTPN2* loss but corrected by tofacitinib

A major feature of IBD is altered cytokine secretion, and especially levels of the inflammatory cytokines TNF- α , IFN- γ and IL-6 as well as levels of IL-22 are highly increased, while the production or the response to the regulatory cytokine IL-10 is compromised in IBD patients.⁵¹ Co-culture of *PTPN2*-deficient macrophages with control Caco-2BBe cells resulted in secretion of IL-6, IL-22, and TNF- α , an effect further enhanced in *PTPN2*-deficient Caco-2BBe cells (Figure 4D, Supplementary Figure 1). Notably, tofacitinib treatment significantly reduced the robust increases in IL-6 and IL-22 (Figure 4D), suggesting that the aberrant secretion of IL-6 and IL-22 upon loss of *PTPN2* in IECs or macrophages may be due to elevated JAK signaling. Loss of *PTPN2* in either cell type, however, had no statistically significant effect on IL-10 secretion and was unaltered by tofacitinib treatment (Figure 4D).

Tofacitinib citrate corrected barrier dysfunction observed in *Ptpn2*-LysMCre mice in vivo

Building on our observations with *in vitro* co-culture models, we next determined whether the restoration of barrier function by tofacitinib translated to an *in vivo* setting using *Ptpn2*-LysMCre mice (lacking *Ptpn2* primarily in monocytes and macrophages⁴⁰) and their *Ptpn2*^{fl/fl} littermates. Consistent with previous findings⁴¹ *Ptpn2*-LysMCre mice exhibited higher *in vivo* FD4 permeability compared to their *Ptpn2*^{fl/fl} counterparts, which was substantially decreased upon twice daily gavage with tofacitinib citrate for 7 d (Figure 5A). In contrast, tofacitinib treatment had no significant effect on FD4 flux in *Ptpn2*^{fl/fl} animals (Figure 5A) suggesting no negative impact on the epithelial barrier upon tofacitinib treatment. Conversely, permeability to creatinine and RD70, which can detect effects on the paracellular pore or the unrestricted pathways, respectively, were not affected by genotype or tofacitinib citrate treatment (Figure 5B+C). Similar to our *in vitro* findings, these data suggest that intestinal permeability is elevated by *PTPN2* loss in macrophages *in vivo*, and this effect can be corrected with JAK-inhibition by tofacitinib.

Tofacitinib rescues the molecular remodeling of tight junctions in IECs from *Ptpn2*-LysMCre mice

To delineate the mechanism behind changes in barrier function *in vivo*, the abundance of tight junction proteins in proximal colon IECs was analyzed. Consistent with previous findings⁴¹ the expression of claudin-2 was significantly increased in IECs from *Ptpn2*-LysMCre mice (Figure 6A+B), while claudin-4, JAM-A, and occludin were all decreased when compared to *Ptpn2*^{fl/fl} controls (Figure 6A-E). These effects were corrected by tofacitinib citrate treatment, and expression patterns of these tight junction proteins were all reversed (Figure 6A-E). Of note

is the induction of occludin expression in *Ptpn2^{fl/fl}* mice by tofacitinib (Figure 6E), though this did not result in changes in FD4 permeability. In contrast, no changes in tricellulin expression were seen as a result of loss of *Ptpn2* in macrophages or tofacitinib citrate treatment (Figure 6F). As described previously, and in line with our *in vitro* data, loss of *Ptpn2* in macrophages promoted the expression of claudin-2 in the crypt regions of *Ptpn2*-LysMCre mice and resulted in reduced and more diffuse E-cadherin and ZO-1 staining (Figure 6G and Supplementary Figure 2). These effects were normalized upon treatment with tofacitinib (Figure 6G and Supplementary Figure 2).

STAT signaling is elevated in IECs of Ptpn2-LysMCre mice, which is effectively reduced by tofacitinib citrate administration

Similar to our cell culture data, *Ptpn2*-deficiency in macrophages also increased STAT3 phosphorylation in IECs *in vivo*, an effect significantly reduced with tofacitinib citrate treatment (Figure 6H). Notably, TCPTP levels remained unchanged in IECs of *Ptpn2^{fl/fl}* vs. *Ptpn2*-LysMCre mice and were unaffected by tofacitinib treatment (Figure 6I). IECs from *Ptpn2*-LysMCre mice did not exhibit elevated STAT1 phosphorylation, suggesting that specific STAT family members are differentially regulated in these animals (Supplementary Figure 3).

Gene and protein expression profiles of cytokines Il6, Il10, and Il22 in Ptpn2-LysMCre colons are reversed by tofacitinib citrate treatment

The local cytokine milieu critically influences epithelial and immune cell processes in the gut. To determine whether loss of *Ptpn2* in macrophages affected the local cytokine milieu in the intestine, *Il6*, *Il10*, and *Il22* gene and protein expression in proximal colon of *Ptpn2^{fl/fl}* and

Ptpn2-LysMCre mice, treated with vehicle or tofacitinib citrate, were determined by qPCR (Figure 7A) and ELISA (Figure 7B). *Il6/Il22* mRNA and IL-6/IL-22 protein expression were significantly elevated, while *Il10* mRNA and IL-10 protein expression were decreased, in vehicle-treated *Ptpn2*-LysMCre mice compared to *Ptpn2*^{fl/fl} mice (Figure 7A+B). With tofacitinib citrate treatment, expression patterns of *Il6/IL-6*, *Il10/IL-10*, and *Il22/IL-22* mRNA and protein levels were reversed, though differences in IL-10 protein expression between vehicle- and tofacitinib citrate-treated *Ptpn2*-LysMCre mice did not reach statistical significance (Figure 7A+B).

Tofacitinib normalizes macrophage polarization profiles in Ptpn2-LysMCre mice

In line with these findings of altered cytokine production, increased proportions of M1 macrophages were observed in *Ptpn2*-LysMCre mice compared to their *Ptpn2*^{fl/fl} counterparts, while M2 macrophage proportions were reduced, with no change in overall macrophage numbers (Figure 7C). Tofacitinib treatment had no effect on M1/M2 macrophage populations in *Ptpn2*^{fl/fl} mice, but reversed the higher M1/lower M2 proportions in *Ptpn2*-LysMCre mice back to approximate ratios found in control mice (Figure 7C). These results confirm that loss of *Ptpn2* affects macrophage polarization, which can be normalized by tofacitinib administration.

Barrier normalization by tofacitinib prevents increased susceptibility to DSS-induced colitis in Ptpn2-LysMCre mice

Finally, we assessed whether correction of barrier defects in *Ptpn2*-LysMCre mice using tofacitinib has consequences for the development of intestinal inflammation. Therefore, *Ptpn2*-LysMCre mice were treated with tofacitinib starting 3 days prior to induction of colitis using

448 1.5% DSS. Pre-treatment with tofacitinib corrected the underlying increase in FD4 permeability
449 in *Ptpn2*-LysMCre mice prior to the start of DSS administration (d0; Figure 8A). Moreover,
450 tofacitinib pre-treatment prevented the DSS-induced increase in FD4 permeability in *Ptpn2*^{fl/fl}
451 and *Ptpn2*-LysMCre mice (d7; Figure 8A). Consistent with previous reports,⁴⁰ vehicle-treated
452 *Ptpn2*-LysMCre mice showed increased colitis severity, as measured by enhanced weight loss,
453 increased disease activity scores, more pronounced shortening of the colon, and elevated
454 histological colitis scores (Figure 8B-F). Notably, these effects were fully prevented by
455 tofacitinib treatment (Figure 8B-D). Furthermore, tofacitinib administration starting 3 days prior
456 to DSS administration also prevented the development of colitis in *Ptpn2*^{fl/fl} mice, as indicated by
457 reduced histological colitis scores (Figure 8E+F).

DISCUSSION

In this study, we identified that tofacitinib corrects the disrupted homeostatic interaction between macrophages and intestinal epithelial cells lacking the IBD risk gene *PTPN2*. Our findings show that tofacitinib normalized barrier dysfunction and changes in tight junction protein expression following loss of *PTPN2* in macrophages and IECs. This intestinal barrier-rescuing effect of tofacitinib was confirmed in mice with myeloid cell-specific knockout of *Ptpn2*. These mice have an underlying, subclinical barrier defect, characterized by increased FD4 permeability associated with reduced expression of tight junction-sealing proteins, elevated epithelial STAT3 activation, altered production of barrier modulating cytokines, increased levels of the pore-forming tight junction molecule claudin-2, and they are more susceptible to DSS-induced colitis.⁴⁰ All these effects were rescued upon treatment with tofacitinib. This demonstrates the clinical relevance of our findings and suggests that loss of functional *PTPN2* in IBD patients, as observed in *PTPN2* loss-of-function variant carriers,^{32,52} might render them more responsive to tofacitinib treatment.

In agreement with previous data,⁴³ *PTPN2*-deficient Caco-2BBE monolayers display much lower TEER and higher FD4 permeability compared to controls, and our data in Figure 1 shows that tofacitinib rescues this effect. Here, we went a step further to demonstrate that tofacitinib rescues intestinal barrier defects caused by disruption of macrophage-IEC interactions upon loss of *PTPN2* in either macrophages or IECs. In our co-culture studies, tofacitinib reversed the expression of some, but not all, tight junction proteins screened, implying that junctional proteins are differentially regulated by the presence of macrophages and/or JAK-STAT signaling in our co-culture system. In addition, since the effects of control and *PTPN2*-deficient THP-1 cells on permeability of Caco-2BBE control monolayers were negated by tofacitinib treatment,

this suggests that tofacitinib-sensitive pathways (presumably JAK-driven) are involved in both the enhancing and detrimental effects of macrophages on IEC barrier function *in vitro*. Of note, there was no adverse effect of tofacitinib citrate treatment on the barrier function of *Ptpn2*^{fl/fl} (wild-type) mice, which implies that *in vivo*, tofacitinib has no detrimental effect on intestinal permeability.

STAT3 and STAT1 phosphorylation in Caco-2BBE cells correlated well with the changes seen in claudin-2 and occludin expression patterns. Disruption of the STAT-binding motif within the *CLDN2* gene promoter prevents aberrantly high *CLDN2* expression observed in *PTPN2* KD IECs,⁴⁴ and increased STAT3 activation in *PTPN2*-deficient IECs promotes claudin-2 expression⁴¹. Whether occludin expression is regulated through JAK-STAT signaling is also not yet known. Surprisingly, the elevated expression of occludin in tofacitinib-treated *Ptpn2*^{fl/fl} mice did not yield a functional decrease in FD4 permeability *in vivo*. The net effect on occludin versus JAM-A (slightly decreased) and tricellulin (no change) expression may thus contribute to the lack of change in macromolecular permeability.

We observed profound changes in the cytokine profile upon loss of *PTPN2*/TCPTP in macrophages and/or epithelial cells, which were corrected by tofacitinib treatment. The strong upregulation of inflammatory cytokines (i.e. IL-6 and TNF α) is well in line with previous reports⁵³ and indicates that TCPTP exerts a critical regulatory function on JAK/STAT signaling to maintain cytokine balance even in the absence of additional stimulation. In specific, we observed increased IL-6 secretion upon *PTPN2* deletion in macrophages, IECs, and in combination. Notably, STAT3 is a major signaling transducer upon IL-6 receptor ligation,⁵⁴ and represents a key downstream target of tofacitinib. Many of the observed effects downstream of *PTPN2* loss can be explained by elevated IL-6 and increased STAT3 activation, but the overall

effect of IL-6 on epithelial barrier function is still under debate.⁵⁵ While 72 h of IL-6 exposure has been shown to decrease TEER and increase mannitol permeability in Caco-2 monolayers,⁵⁶ 4 kDa-dextran permeability was increased in IL-6 knockout mice when compared to controls,⁵⁷ Thus, IL-6 has pleiotropic functions and while some of the observed effects might result from elevated IL-6 in *Ptpn2*-LysMCre mice,⁴¹ there are likely other factors that contribute to the decreased TEER/barrier function upon loss of *PTPN2* in IEC or macrophages. In line with this, we observed that the secretion pattern of TNF- α in our co-culture studies was similar to that of IL-6. TNF- α can induce IL-6 production in Caco-2 cells⁵⁸ and, in combination with IFN- γ , in THP-1 cells,⁵⁹ and thus might be responsible for the elevated IL-6 levels observed here. Epithelial and immune cells produce IL-6,⁶⁰ therefore, the changes we observed in tight junction proteins and JAK-STAT activation could result from autocrine or paracrine signaling. In our co-culture experiments, tofacitinib reduced IL-6 and TNF- α secretion, which agrees with recent findings that tofacitinib pretreatment reduced both IL-6 and TNF- α secretion in human peripheral monocytes.¹⁶

The profound changes in the expression profiles of IL-6, IL-22, and IL-10 upon loss of TCPTP, which were partially rescued upon tofacitinib treatment, yield insight into which mediators may be causing the changes observed in mice treated with tofacitinib citrate. The elevated expression of the pro-inflammatory cytokine IL-6 and reduced expression of anti-inflammatory IL-10 in proximal colons of vehicle-treated *Ptpn2*-LysMCre mice suggest that at basal levels, the intestines of these mice are primed towards a pro-inflammatory phenotype. Furthermore, and in agreement with findings that IL-22 upregulates claudin-2 to increase water efflux for bacterial clearance,⁴⁷ both IL-6 and IL-22 protein secretion and mRNA expression correlated with claudin-2 levels. *IL22* mRNA expression is also elevated in active CD⁶¹ and

UC,⁶² and has been shown to promote epithelial restitution in wound-healing assays,⁶¹ and attenuate intestinal inflammation *in vivo*.⁶³

Oral gavage of molecular probes such as FD4 and RD70, and assessment of their serum levels, allows for functional analysis of intestinal permeability *in vivo*.⁴⁷ In this approach, unaltered permeability to RD70 confirmed the absence of mucosal damage in *Ptpn2*-LysMCre mice, while increased FD4 flux demonstrated an increase in the leak pathway, which allows smaller macromolecules, such as bacterial products, to pass through the epithelial paracellular barrier and elicit an immune response. Importantly, this effect was reversed upon tofacitinib citrate treatment, indicating that this drug can normalize barrier defects elicited by macrophages with a pro-inflammatory phenotype. Furthermore, and in agreement with a recent study demonstrating that tofacitinib pretreatment skews murine BMDMs towards a regulatory, M2-like phenotype,¹⁴ tofacitinib reversed the enhanced M1 macrophage levels in *Ptpn2*-LysMCre mice and restored M2 macrophage proportions. Together with our co-culture studies, this effect of tofacitinib on macrophage polarization indicates a novel mechanism by which JAK inhibition protects the intestinal epithelium. Of note, this protective effect on barrier permeability and correction of macrophage phenotype had direct consequences for the enhanced susceptibility to intestinal inflammation observed in *Ptpn2*-LysMCre mice, which was completely rescued upon tofacitinib administration. One notable difference from the De Vries study¹⁴ is that we observed inhibition of onset of DSS colitis symptoms by tofacitinib citrate pretreatment, albeit starting 3 days prior to DSS vs. concurrent administration. Our results not only suggests that the detrimental effects of *PTPN2*-deficient macrophages on IEC barrier function is relevant for the development of intestinal inflammation, but also indicates that tofacitinib can restore barrier function and revert the enhanced colitis susceptibility of mice lacking *PTPN2* in macrophages.

Moreover, the protective effect when administered prior to disease induction indicates that tofacitinib treatment might be a promising candidate to maintain remission in UC patients and especially in those with *PTPN2* loss-of-function variants.

The genetic profiles of IBD patients included in tofacitinib clinical studies were not reported and thus it is still unknown whether genetic factors determine treatment success. Our results with macrophages and IECs lacking the IBD risk gene *PTPN2*, suggest that analyzing subgroups of patients with distinct genetic profiles for their response to tofacitinib might be a promising approach to detect patients that are more responsive for tofacitinib treatment. Adverse events such as increased rates of overall infections, herpes zoster infections, cardiovascular events, and increased serum lipid levels were observed in IBD patients who received tofacitinib treatment for 52 weeks,¹² and higher rates of pulmonary embolisms and mortality have occurred in rheumatoid arthritis patients receiving high (10 mg) amounts of tofacitinib.⁶⁴ Given the potential for side effects, specifically selecting patients who might be genetically predisposed to respond more favorably to tofacitinib treatment would represent a crucial advance in treating IBD and other autoimmune diseases.

In summary, our results demonstrate that tofacitinib treatment corrected barrier function and tight junction regulation in a co-culture system of IECs with *PTPN2*-deficient inflammatory macrophages, as well as in an *in vivo* model system reflecting disrupted macrophage-IEC crosstalk upon loss of *Ptpn2* in macrophages, and was able to revert enhanced colitis susceptibility in mice with macrophage-specific *Ptpn2* deletion. Our work integrates studies demonstrating effects of tofacitinib on macrophages alone with a major physiological role for these innate immune cells in the regulation of intestinal epithelial barrier function. Our findings indicate that tofacitinib treatment might be an especially effective treatment to restore barrier

function and maintain remission in patients harboring *PTPN2* loss-of-function mutations. In addition, the presence of *PTPN2* variants might be a good predictor for treatment response to tofacitinib not only in approved conditions like ulcerative colitis, but also in patients not currently indicated for treatment with tofacitinib, such as those with Crohn's disease. Given the recent important findings demonstrating that increased intestinal permeability is significantly associated with the future risk of developing Crohn's disease, our data make a potentially significant contribution to the discovery of new agents that can be used to prevent IBD onset by promoting and maintaining a healthy gut barrier.²⁶ Since *PTPN2* variants are not only associated with an increased risk to develop IBD, but also with a number of other inflammatory disorders, our findings might not only be relevant for patients suffering from intestinal inflammation, but also for patients suffering from other disease entities that are associated with *PTPN2* variants in which tofacitinib represents an established therapy (e.g. rheumatoid arthritis), or where it might be considered as a therapeutic strategy in the future.

CONFLICT OF INTEREST

The authors declare no conflict of interest.

AUTHORS CONTRIBUTION

MRS, AS-B: experiment design, data acquisition, analysis, and interpretation, writing of the manuscript; CO, VC, ANS, SK: data acquisition and analysis; MK: generation of lentiviral constructs for *PTPN2*-specific and scrambled shRNA; MGN: critical input on flow cytometry, MS: data interpretation and critical intellectual input; DFM, MRS: data interpretation, study design, funding, editing of the manuscript. All authors wrote, revised and approved the manuscript.

REFERENCES

1. Adams SM, Bornemann PH. Ulcerative colitis. *Am Fam Physician* 2013;**87**:699-705.
2. Ordas I, Eckmann L, Talamini M, Baumgart DC, Sandborn WJ. Ulcerative colitis. *Lancet* 2012;**380**:1606-19.
3. Baumgart DC, Sandborn WJ. Crohn's disease. *Lancet* 2012;**380**:1590-605.
4. Kaser A, Zeissig S, Blumberg RS. Inflammatory bowel disease. *Annu Rev Immunol* 2010;**28**:573-621.
5. Danese S, Fiorino G, Peyrin-Biroulet L, *et al.* Biological agents for moderately to severely active ulcerative colitis: A systematic review and network meta-analysis. *Ann Intern Med* 2014;**160**:704-11.
6. Danese S, Fiorino G, Peyrin-Biroulet L. Early intervention in crohn's disease: Towards disease modification trials. *Gut* 2017;**66**:2179-87.
7. Gisbert JP, Marin AC, Chaparro M. The risk of relapse after anti-tnf discontinuation in inflammatory bowel disease: Systematic review and meta-analysis. *Am J Gastroenterol* 2016;**111**:632-47.
8. Gisbert JP, Marin AC, Chaparro M. Systematic review: Factors associated with relapse of inflammatory bowel disease after discontinuation of anti-tnf therapy. *Aliment Pharmacol Ther* 2015;**42**:391-405.
9. Baert F, Noman M, Vermeire S, *et al.* Influence of immunogenicity on the long-term efficacy of infliximab in crohn's disease. *N Engl J Med* 2003;**348**:601-8.
10. Dhillon S. Tofacitinib: A review in rheumatoid arthritis. *Drugs* 2017;**77**:1987-2001.
11. Berekmeri A, Mahmood F, Wittmann M, Helliwell P. Tofacitinib for the treatment of psoriasis and psoriatic arthritis. *Expert Rev Clin Immunol* 2018;**14**:719-30.
12. Sandborn WJ, Su C, Sands BE, *et al.* Tofacitinib as induction and maintenance therapy for ulcerative colitis. *N Engl J Med* 2017;**376**:1723-36.
13. Inc. P. Pfizer announces u.S. Fda approves xeljanz® (tofacitinib) for the treatment of moderately to severely active ulcerative colitis.
<https://www.pfizer.com/news/press-release/press-release-detail/pfizer-announces-u-s-fda-approves-xeljanz-tofacitinib-for-the-treatment-of-moderately-to-severely-active-ulcerative-colitis-0>.: Pfizer, 2019.
14. De Vries LCS, Duarte JM, De Krijger M, *et al.* A jak1 selective kinase inhibitor and tofacitinib affect macrophage activation and function. *Inflamm Bowel Dis* 2019;**25**:647-60.
15. Beattie DT, Pulido-Rios MT, Shen F, *et al.* Intestinally-restricted janus kinase inhibition: A potential approach to maximize the therapeutic index in inflammatory bowel disease therapy. *J Inflamm (Lond)* 2017;**14**:28.
16. Cordes F, Lenker E, Spille LJ, *et al.* Tofacitinib reprograms human monocytes of ibd patients and healthy controls toward a more regulatory phenotype. *Inflamm Bowel Dis* 2020;**26**:391-406.
17. Garcia-Hernandez V, Quiros M, Nusrat A. Intestinal epithelial claudins: Expression and regulation in homeostasis and inflammation. *Ann N Y Acad Sci* 2017;**1397**:66-79.

18. Buckley A, Turner JR. Cell biology of tight junction barrier regulation and mucosal disease. *Cold Spring Harb Perspect Biol* 2018;**10**.
19. Clayburgh DR, Shen L, Turner JR. A porous defense: The leaky epithelial barrier in intestinal disease. *Lab Invest* 2004;**84**:282-91.
20. Odenwald MA, Turner JR. The intestinal epithelial barrier: A therapeutic target? *Nat Rev Gastroenterol Hepatol* 2017;**14**:9-21.
21. Irvine EJ, Marshall JK. Increased intestinal permeability precedes the onset of crohn's disease in a subject with familial risk. *Gastroenterology* 2000;**119**:1740-4.
22. Olson TS, Reuter BK, Scott KG, *et al*. The primary defect in experimental ileitis originates from a nonhematopoietic source. *J Exp Med* 2006;**203**:541-52.
23. Wyatt J, Vogelsang H, Hubl W, Waldhoer T, Lochs H. Intestinal permeability and the prediction of relapse in crohn's disease. *Lancet* 1993;**341**:1437-9.
24. D'Inca R, Di Leo V, Corrao G, *et al*. Intestinal permeability test as a predictor of clinical course in crohn's disease. *Am J Gastroenterol* 1999;**94**:2956-60.
25. Hollander D, Vadheim CM, Brettholz E, *et al*. Increased intestinal permeability in patients with crohn's disease and their relatives. A possible etiologic factor. *Ann Intern Med* 1986;**105**:883-5.
26. Turpin W, Lee S-H, Raygoza Garay JA, *et al*. Increased intestinal permeability is associated with later development of crohn's disease. *Gastroenterology* 2020.
27. Wellcome Trust Case Control C. Genome-wide association study of 14,000 cases of seven common diseases and 3,000 shared controls. *Nature* 2007;**447**:661-78.
28. Liu JZ, van Sommeren S, Huang H, *et al*. Association analyses identify 38 susceptibility loci for inflammatory bowel disease and highlight shared genetic risk across populations. *Nat Genet* 2015;**47**:979-86.
29. de Lange KM, Moutsianas L, Lee JC, *et al*. Genome-wide association study implicates immune activation of multiple integrin genes in inflammatory bowel disease. *Nat Genet* 2017;**49**:256-61.
30. Jostins L, Ripke S, Weersma RK, *et al*. Host-microbe interactions have shaped the genetic architecture of inflammatory bowel disease. *Nature* 2012;**491**:119-24.
31. Long SA, Cerosaletti K, Wan JY, *et al*. An autoimmune-associated variant in ptpn2 reveals an impairment of il-2r signaling in cd4(+) t cells. *Genes Immun* 2011;**12**:116-25.
32. Scharl M, Mwinyi J, Fischbeck A, *et al*. Crohn's disease-associated polymorphism within the ptpn2 gene affects muramyl-dipeptide-induced cytokine secretion and autophagy. *Inflamm Bowel Dis* 2012;**18**:900-12.
33. Parlato M, Nian Q, Charbit-Henrion F, *et al*. Loss of function mutation in ptpn2 causes aberrant activation of jak signaling via stat and very early onset intestinal inflammation. *Gastroenterology* 2020.
34. Simoncic PD, Bourdeau A, Lee-Loy A, *et al*. T-cell protein tyrosine phosphatase (tcptp) is a negative regulator of colony-stimulating factor 1 signaling and macrophage differentiation. *Mol Cell Biol* 2006;**26**:4149-60.
35. McCole DF. Regulation of epithelial barrier function by the inflammatory bowel disease candidate gene, ptpn2. *Ann N Y Acad Sci* 2012;**1257**:108-14.
36. Shuai K, Liu B. Regulation of jak-stat signalling in the immune system. *Nat Rev Immunol* 2003;**3**:900-11.

37. You-Ten KE, Muise ES, Itie A, *et al.* Impaired bone marrow microenvironment and immune function in t cell protein tyrosine phosphatase-deficient mice. *J Exp Med* 1997;**186**:683-93.
38. Scharl M, Paul G, Weber A, *et al.* Protection of epithelial barrier function by the crohn's disease associated gene protein tyrosine phosphatase n2. *Gastroenterology* 2009;**137**:2030-40 e5.
39. Spalinger MR, Kasper S, Chassard C, *et al.* Ptpn2 controls differentiation of cd4(+) t cells and limits intestinal inflammation and intestinal dysbiosis. *Mucosal Immunol* 2015;**8**:918-29.
40. Spalinger MR, Manzini R, Hering L, *et al.* Ptpn2 regulates inflammasome activation and controls onset of intestinal inflammation and colon cancer. *Cell Rep* 2018;**22**:1835-48.
41. Spalinger MR, Sayoc-Becerra A, Santos AN, *et al.* Ptpn2 regulates interactions between macrophages and intestinal epithelial cells to promote intestinal barrier function. *Gastroenterology* 2020.
42. Sayoc-Becerra A, Krishnan M, Fan S, *et al.* The jak-inhibitor tofacitinib rescues human intestinal epithelial cells and colonoids from cytokine-induced barrier dysfunction. *Inflamm Bowel Dis* 2020;**26**:407-22.
43. Krishnan M, Penrose HM, Shah NN, Marchelletta RR, McCole DF. Vsl#3 probiotic stimulates t-cell protein tyrosine phosphatase-mediated recovery of ifn-gamma-induced intestinal epithelial barrier defects. *Inflamm Bowel Dis* 2016;**22**:2811-23.
44. Krishnan M, McCole DF. T cell protein tyrosine phosphatase prevents stat1 induction of claudin-2 expression in intestinal epithelial cells. *Ann N Y Acad Sci* 2017;**1405**:116-30.
45. Schneider CA, Rasband WS, Eliceiri KW. Nih image to imagej: 25 years of image analysis. *Nat Methods* 2012;**9**:671-5.
46. Clausen BE, Burkhardt C, Reith W, Renkawitz R, Forster I. Conditional gene targeting in macrophages and granulocytes using lysmcre mice. *Transgenic Res* 1999;**8**:265-77.
47. Tsai PY, Zhang B, He WQ, *et al.* Il-22 upregulates epithelial claudin-2 to drive diarrhea and enteric pathogen clearance. *Cell Host Microbe* 2017;**21**:671-81 e4.
48. Shawki A, Ramirez R, Spalinger MR, *et al.* The autoimmune susceptibility gene, ptpn2, restricts expansion of a novel mouse adherent-invasive e. Coli. *Gut Microbes* 2020;**11**:1547-66.
49. Shen L, Weber CR, Raleigh DR, Yu D, Turner JR. Tight junction pore and leak pathways: A dynamic duo. *Annu Rev Physiol* 2011;**73**:283-309.
50. Heinemann U, Schuetz A. Structural features of tight-junction proteins. *Int J Mol Sci* 2019;**20**.
51. Muzes G, Molnar B, Tulassay Z, Sipos F. Changes of the cytokine profile in inflammatory bowel diseases. *World J Gastroenterol* 2012;**18**:5848-61.
52. Marcil V, Mack DR, Kumar V, *et al.* Association between the ptpn2 gene and crohn's disease: Dissection of potential causal variants. *Inflamm Bowel Dis* 2013;**19**:1149-55.
53. Scharl M, Hruz P, McCole DF. Protein tyrosine phosphatase non-receptor type 2 regulates ifn-gamma-induced cytokine signaling in thp-1 monocytes. *Inflamm Bowel Dis* 2010;**16**:2055-64.

54. Wang Y, van Boxel-Dezaire AH, Cheon H, Yang J, Stark GR. Stat3 activation in response to il-6 is prolonged by the binding of il-6 receptor to egf receptor. *Proc Natl Acad Sci U S A* 2013;**110**:16975-80.
55. Al-Sadi R, Boivin M, Ma T. Mechanism of cytokine modulation of epithelial tight junction barrier. *Front Biosci (Landmark Ed)* 2009;**14**:2765-78.
56. Tazuke Y, Drongowski RA, Teitelbaum DH, Coran AG. Interleukin-6 changes tight junction permeability and intracellular phospholipid content in a human enterocyte cell culture model. *Pediatr Surg Int* 2003;**19**:321-5.
57. Wang L, Srinivasan S, Theiss AL, Merlin D, Sitaraman SV. Interleukin-6 induces keratin expression in intestinal epithelial cells: Potential role of keratin-8 in interleukin-6-induced barrier function alterations. *J Biol Chem* 2007;**282**:8219-27.
58. Vitkus SJ, Hanifin SA, McGee DW. Factors affecting caco-2 intestinal epithelial cell interleukin-6 secretion. *In Vitro Cell Dev Biol Anim* 1998;**34**:660-4.
59. Sanceau J, Wijdenes J, Revel M, Wietzerbin J. Il-6 and il-6 receptor modulation by ifn-gamma and tumor necrosis factor-alpha in human monocytic cell line (thp-1). Priming effect of ifn-gamma. *J Immunol* 1991;**147**:2630-7.
60. Song M, Kellum JA. Interleukin-6. *Crit Care Med* 2005;**33**:S463-5.
61. Brand S, Beigel F, Olszak T, *et al.* Il-22 is increased in active crohn's disease and promotes proinflammatory gene expression and intestinal epithelial cell migration. *Am J Physiol Gastrointest Liver Physiol* 2006;**290**:G827-38.
62. Yamamoto-Furusho JK, Miranda-Perez E, Fonseca-Camarillo G, *et al.* Colonic epithelial upregulation of interleukin 22 (il-22) in patients with ulcerative colitis. *Inflamm Bowel Dis* 2010;**16**:1823.
63. Sugimoto K, Ogawa A, Mizoguchi E, *et al.* Il-22 ameliorates intestinal inflammation in a mouse model of ulcerative colitis. *J Clin Invest* 2008;**118**:534-44.
64. FDA. Fda approves boxed warning about increased risk of blood clots and death with higher dose of arthritis and ulcerative colitis medicine tofacitinib (xeljanz, xeljanz xr). <https://www.fda.gov/drugs/drug-safety-and-availability/fda-approves-boxed-warning-about-increased-risk-blood-clots-and-death-higher-dose-arthritis-and>. Accessed December 5, 2019.

FIGURE LEGENDS

Figure 1: Tofacitinib corrects barrier defects caused by loss of *PTPN2* in intestinal epithelial cells and macrophages. A) Transepithelial electrical resistance (TEER) and B) 4 kDa fluorescein-dextran (FD4) flux across Caco-2BBE monolayers pretreated with vehicle (0.5% DMSO) or tofacitinib (Tofa, 50 μ M) for 1 hour prior to co-culture with control (Ctr) or *PTPN2* knockdown (KD) THP-1 macrophages for 24 hours. * $P \leq 0.05$ *cf.* vehicle-treated control Caco-2BBE without co-culture; # $P \leq 0.05$ *cf.* vehicle-treated Ctr Caco-2BBE with Ctr macrophages; § $P \leq 0.05$ *cf.* vehicle Ctr Caco-2BBE with KD macrophages, x $P \leq 0.05$ *cf.* vehicle-treated KD Caco-2BBE without macrophages, ¶ $P \leq 0.05$ *cf.* vehicle-treated KD Caco-2BBE with control macrophages, o $P \leq 0.05$ *cf.* vehicle-treated Ctr Caco-2BBE with KD macrophages; $n = 3$. The “—” symbol indicates no co-culture.

Figure 2: Tofacitinib normalizes tight junction protein expression in Caco-2BBE cells mediated by *PTPN2* loss in IECs and/or macrophages. Caco-2BBE monolayers pretreated with vehicle (0.5% DMSO) or tofacitinib (Tofa, 50 μ M) for 1 hour prior to co-culture with control (Ctr) or *PTPN2* knockdown (KD) THP-1 cells for 24 hours were lysed and subjected to Western blotting. A) Representative Western blot images of the indicated proteins from Caco-2BBE whole cell lysates. Densitometric analyses of B) claudin-2, C) claudin-4, D) JAM-A, E) occludin, F) tricellulin, and G) TCPTP expression, all normalized to β -actin; H) Caco-2 cells were grown on cover slides and pretreated with tofacitinib before addition of conditioned medium from Ctr or KD THP-1 cells for 24 hours and subsequent immunofluorescence staining for ZO-1. Arrows point to regions with ZO-1 internalization. Scale bar: 10 μ m * $P \leq 0.05$, ** $P \leq 0.01$, **** $P \leq 0.0001$ *cf.* vehicle-treated Ctr Caco-2BBE without co-culture; # $P \leq 0.05$, ## $P \leq$

0.01, ### $P \leq 0.001$, #### $P \leq 0.0001$ *cf.* ; # $P \leq 0.05$ *cf.* vehicle-treated Ctr Caco-2BBe with Ctr macrophages; § $P \leq 0.05$, §§ $P \leq 0.01$ *cf.* vehicle Ctr Caco-2BBe with KD macrophages, x $P \leq 0.05$ *cf.* vehicle-treated KD Caco-2BBe without macrophages, ¶ $P \leq 0.05$ *cf.* vehicle-treated KD Caco-2BBe with Ctr macrophages, • $P \leq 0.05$ *cf.* vehicle-treated Ctr Caco-2BBe with KD macrophages; $n = 3$. The “–” symbol indicates no co-culture.

Figure 3: Functional inhibition of STAT signaling by tofacitinib in Caco-2BBe cells co-cultured with macrophages. Caco-2BBe monolayers pretreated with vehicle (0.5% DMSO) or tofacitinib (Tofa, 50 μ M) for 1 hour prior to co-culture with control (Ctr) or *PTPN2* knockdown (KD) THP-1 cells for 24 hours. Representative Western blot images and densitometric analyses of A) phospho-STAT1 (pSTAT1) and B) phospho-STAT3 (pSTAT3) normalized to their respective total forms (tSTAT1, tSTAT3) in Caco-2BBe whole cell lysates. * $P \leq 0.05$, **** $P \leq 0.0001$ *cf.* vehicle-treated Ctr Caco-2BBe without co-culture; ## $P \leq 0.01$ *cf.* vehicle-treated Ctr Caco-2BBe with Ctr macrophages; §§ $P \leq 0.01$, §§§ $P \leq 0.001$ *cf.* vehicle Ctr Caco-2BBe with KD macrophages, xx $P \leq 0.01$, xxx $P \leq 0.01$ *cf.* vehicle-treated KD Caco-2BBe without macrophages, ¶¶ $P \leq 0.01$, ¶¶¶ $P \leq 0.001$ *cf.* vehicle-treated KD Caco-2BBe with Ctr macrophages, oo $P \leq 0.01$, ooo $P \leq 0.001$ *cf.* vehicle-treated Ctr Caco-2BBe with KD macrophages; $n = 3$. The “–” symbol indicates no co-culture.

Figure 4: Tofacitinib reduces STAT signaling in THP-1 macrophages and cytokine IL-6 secretion in co-culture studies. THP-1 macrophages co-cultured with tofacitinib-treated Caco-2BBe cells for 24 hours were lysed and subjected to Western blotting. Representative Western blot images and densitometric analyses of A) phospho-JAK1 (pJAK1), B) phospho-STAT1

(pSTAT1) and C) phospho-STAT3 (pSTAT3) normalized to their respective total forms (tJAK1, tSTAT1, tSTAT3) in THP-1 whole cell lysates. D) IL-6, IL-22, and IL-10 concentrations present in the culture media after co-culture experiments, measured by ELISA. * $P \leq 0.05$, *** $P \leq 0.001$ *cf.* vehicle-treated Ctr THP-1 without co-culture; § $P \leq 0.05$, §§ $P \leq 0.01$, §§§ $P \leq 0.001$ *cf.* vehicle-treated Ctr THP-1 with KD Caco-2BBE, x $P \leq 0.05$, xx $P \leq 0.01$, xxx $P \leq 0.01$ *cf.* vehicle-treated KD THP-1 without co-culture, ¶ $P \leq 0.05$, ¶¶¶ $P \leq 0.001$ *cf.* vehicle-treated KD THP-1 without co-culture, o $P \leq 0.05$, ooo $P \leq 0.001$ *cf.* vehicle-treated Ctr THP-1 with Ctr Caco-2BBE; $n = 3$. The “—” symbol indicates no co-culture.

Figure 5: Tofacitinib citrate treatment reduced barrier permeability to FD4 *in vivo*.

Intestinal permeability to creatinine, FD4, and RD70 was measured in *Ptpn2*^{fl/fl} and *Ptpn2*-LysMCre mice subjected to twice daily treatment with vehicle (1% methylcellulose in PBS) or tofacitinib citrate (50 mg/kg) for 7 days. Serum concentrations of A) FD4, B) creatinine, and C) RD70 were measured 5 hours post-gavage. * $P \leq 0.05$; $n = 6$ per group, representative results of two independent experiments.

Figure 6: Aberrant tight junction protein patterns and elevated STAT3 phosphorylation in

***Ptpn2*-LysMCre mice were reversed upon tofacitinib citrate treatment.** Whole cell lysates of proximal colon IECs isolated from *Ptpn2*^{fl/fl} and *Ptpn2*-LysMCre mice treated with vehicle or tofacitinib citrate (Tofa) for 7 days were subjected to Western blot analysis. A) Representative Western blot images and respective densitometric analyses of B) claudin-2, C) claudin-4, D) JAM-A, E) occludin, F) tricellulin, normalized to β -actin. G) Immunofluorescence staining for ZO-1 (white), E-cadherin (red), and claudin-2 (green) in colon sections from *Ptpn2*^{fl/fl} and *Ptpn2*-

LysMCre mice treated with vehicle or tofacitinib citrate for 7 days. White arrows indicate cell border localization of ZO-1, green arrow cell border localization of claudin-2. See also Supplementary Figure S2. Densitometric analysis of H) phospho-STAT3 (pSTAT3) normalized to total STAT3 (tSTAT3) and I) TCPTP normalized to β -actin. $*P \leq 0.05$, $**P \leq 0.01$, $***P \leq 0.001$; $n = 6$ per group, representative results of two independent experiments.

Figure 7: Cytokine production and macrophage polarization are normalized by tofacitinib citrate treatment in *Ptpn2*-LysMCre mice. A) mRNA expression of *Il6*, *Il10*, and *Il22* normalized to *Gapdh* in whole proximal colons of mice treated with vehicle or tofacitinib citrate twice daily for 7 days. B) Protein expression of IL-6, IL-10, and IL-22 as determined by ELISA. C) Proportions of total macrophages (CD11b⁺, Ly6G⁻, F4/80⁺, CD64⁺ cells), M1 (CD86 high, CD206 low), and M2 (CD86 low, CD206 high) macrophages in whole proximal colons of mice as determined by flow cytometry (all cells were pre-gated on live, single, CD45⁺ cells). $*P \leq 0.05$, $**P \leq 0.01$, $***P \leq 0.001$, $****P \leq 0.0001$; $n = 6$ per group, representative results of two independent experiments.

Figure 8: Tofacitinib citrate treatment prevents colitis in *Ptpn2*-LysMCre mice. *Ptpn2*-LysMCre and *Ptpn2*^{fl/fl} mice were treated twice daily with tofacitinib citrate starting 3 days before exposure to 1.5% DSS in the drinking water for 7 days. A) FD4 permeability at the start of the experiment (d-3), at the day of DSS start (d0) and at the end of the experiment (d7). B) Weight development, C) disease activity score, D) colon length, E) representative pictures from H&E stained terminal colon sections, and F) respective histological scoring of colitis severity. Scale bars: 100 μ m. $*P \leq 0.05$, $**P \leq 0.01$; $n = 4$ per group.

Supplementary Figure 1: Tofacitinib partially reduces pro-inflammatory cytokine TNF- α secretion in co-culture studies. TNF- α levels present in the culture media after co-culture experiments as measured by ELISA. * $P \leq 0.05$, *** $P \leq 0.001$ *cf.* untreated Ctr THP-1; # $P \leq 0.05$, ## $P \leq 0.01$ *cf.* vehicle-treated THP-1; $n = 3$.

Supplementary Figure 2: Tofacitinib citrate treatment reduces claudin-2 expression in *Ptpn2*-LysMCre mice and normalizes localization of ZO-1 to the cell membrane. Immunofluorescence staining for ZO-1, E-cadherin, and claudin-2 on colon sections from *Ptpn2*^{fl/fl} and *Ptpn2*-LysMCre mice treated with vehicle or tofacitinib citrate for 7 days. White squares indicate pictures shown in main Figure 6G.

Supplementary Figure 3: Tofacitinib does not affect STAT1 phosphorylation in IECs from *Ptpn2*-LysMCre mice *in vivo*. Lysates of proximal colon IECs isolated from *Ptpn2*^{fl/fl} and *Ptpn2*-LysMCre mice treated with vehicle or tofacitinib citrate were analyzed for STAT1 phosphorylation by Western blot. $n = 6$ per group, representative results for one of two independent experiments. Related to main Figure 6.

877 **SUPPLEMENTARY TABLES:**878 **Supplementary Table 1: Primary and secondary antibodies for Western blotting**

Antibody	Host	Provider	Catalog No.	Dilution
Claudin-2	Mouse	Thermo Fisher Scientific (Rockford, IL)	32-5600	1:1000
Claudin-4	Mouse	Invitrogen (Camarillo, CA)	32-9400	1:1000
JAM-A	Rabbit	Invitrogen (Camarillo, CA)	36-1700	1:1000
Occludin	Rabbit	Thermo Fisher Scientific (Rockford, IL)	71-1500	1:1000
Tricellulin (MARVELD2)	Rabbit	Abcam	ab203567	1:1000
TCPTP (anti-mouse)	Mouse	Medimabs (Quebec, Canada)	MM-0018	1:500
TCPTP (anti-human)	Mouse	EMD Millipore (San Diego, CA)	PH03L	1:500
Phospho-JAK1 (Tyr 1022/1023)	Rabbit	Cell Signaling Technology (Danvers, MA)	#3331	1:1000
Total JAK1	Rabbit	Cell Signaling Technology (Danvers, MA)	#3344	1:1000
Phospho-STAT1 (Tyr 701)	Rabbit	Cell Signaling Technology (Danvers, MA)	#9167	1:1000
Total STAT1	Rabbit	Cell Signaling Technology (Danvers, MA)	#9175	1:1000
Phospho-STAT3 (Tyr 705)	Rabbit	Cell Signaling Technology (Danvers, MA)	#9145	1:1000
Total STAT3	Mouse	Cell Signaling Technology (Danvers, MA)	#9139	1:2000
β -actin	Mouse	Sigma Aldrich	A5316	1:5000
HRP-conjugated anti-rabbit IgG	Goat	Jackson ImmunoResearch Laboratories, Inc. (West Grove, PA)	#111-036-045	1:3000
HRP-conjugated anti-mouse IgG	Goat	Jackson ImmunoResearch Laboratories, Inc. (West Grove, PA)	#115-036-062	1:3000

879

880

Supplementary Table 2: Fluorescence-labeled antibodies used for flow cytometry

Antibody	Fluorophore	Host, Isotype	Provider	Catalog No.	Clone	Dilution
CD11b (mouse)	BV605	Rat IgG2b κ	Biolegend	101237	M1/70	1:200
Ly-6G (mouse)	BV510	Rat IgG2a κ	Biolegend	127633	1A8	1:100
Ly-6C (mouse)	PerCP/Cy5.5	Rat IgG2c κ	BioLegend	128011	HK1.4	1:200
CD11c (mouse)	PE/Cy7	Hms IgG	Biolegend	117318	N418	1:200
MHC-II (mouse)	AF700	Rat IgG2b κ	Thermo Fisher	56-5321-80	M5/114.15.2	1:100
CD64 (mouse)	PE	Ms IgG1 κ	BioLegend	139303	X54-5/7.1	1:200
CD45 (mouse)	PB	Rat IgG2b κ	BioLegend	103125	30-F11	1:400
F4/80 (mouse)	APC	Rat IgG2a κ	BioLegend	123115	BM8	1:200
CD3 (mouse)	BV650	Rat IgG2b κ	Biolegend	100229	17A2	1:400
NK-1.1 (mouse)	BV650	Ms IgG2a κ	BioLegend	108735	PK136	1:200
CD45R/B220 (mouse/human)	PE/Cy5	Rat IgG2a κ	Biolegend	103209	RA3-6B2	1:400
CD206 (mouse)	PE	Rat IgG2a κ	Biolegend	141705	C068C2	1:100
CD86 (mouse)	AF488	Rat IgG2a κ	Biolegend	105018	GL-1	1:100
Fc block (mouse)	-	several	Miltenyi Biotec	130-092-575	several	1:100

881

882 **Supplementary Table 3: Primer sequences used for quantitative PCR**

Primers	Forward	Reverse
<i>Il6</i>	AGTCCGGAGAGGAGACTTCA	TTGCCATTGCACAACTCTTT
<i>Il10</i>	CCCAGAAATCAAGGAGCATT	TCACTCTTCACCTGCTCCAC
<i>Il22</i>	GCTCAGCTCCTGTCACATCA	CAGTTCCCCAATCGCCTTGA
<i>Gapdh</i>	CATCACTGCCACCCAGAAGACTG	ATGCCAGTGAGCTTCCCGTTCAG

883

884

885

FIGURE 1

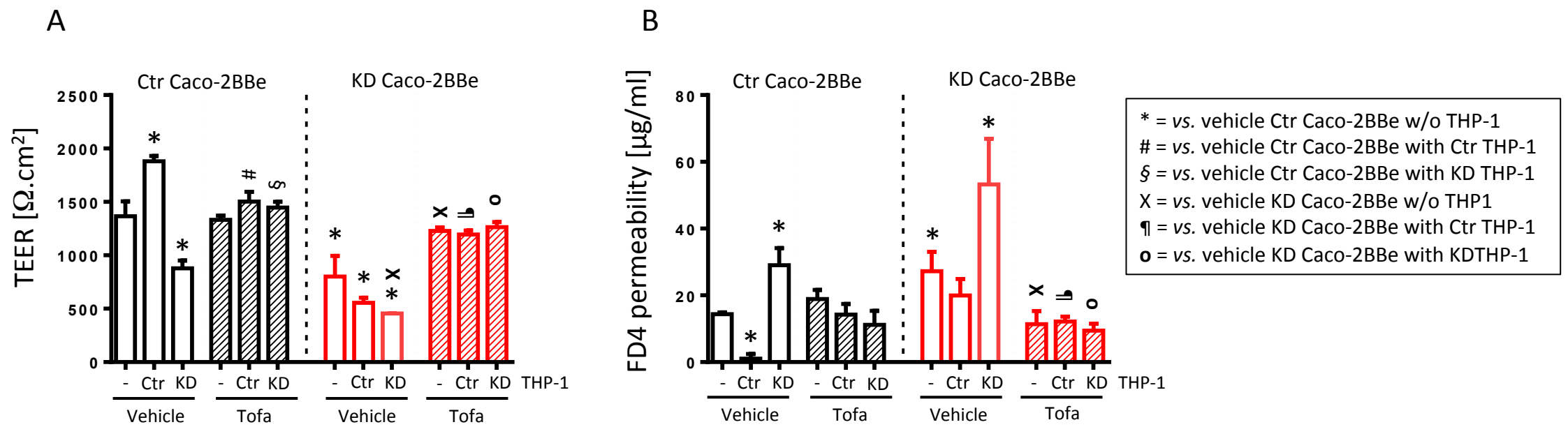


FIGURE 2

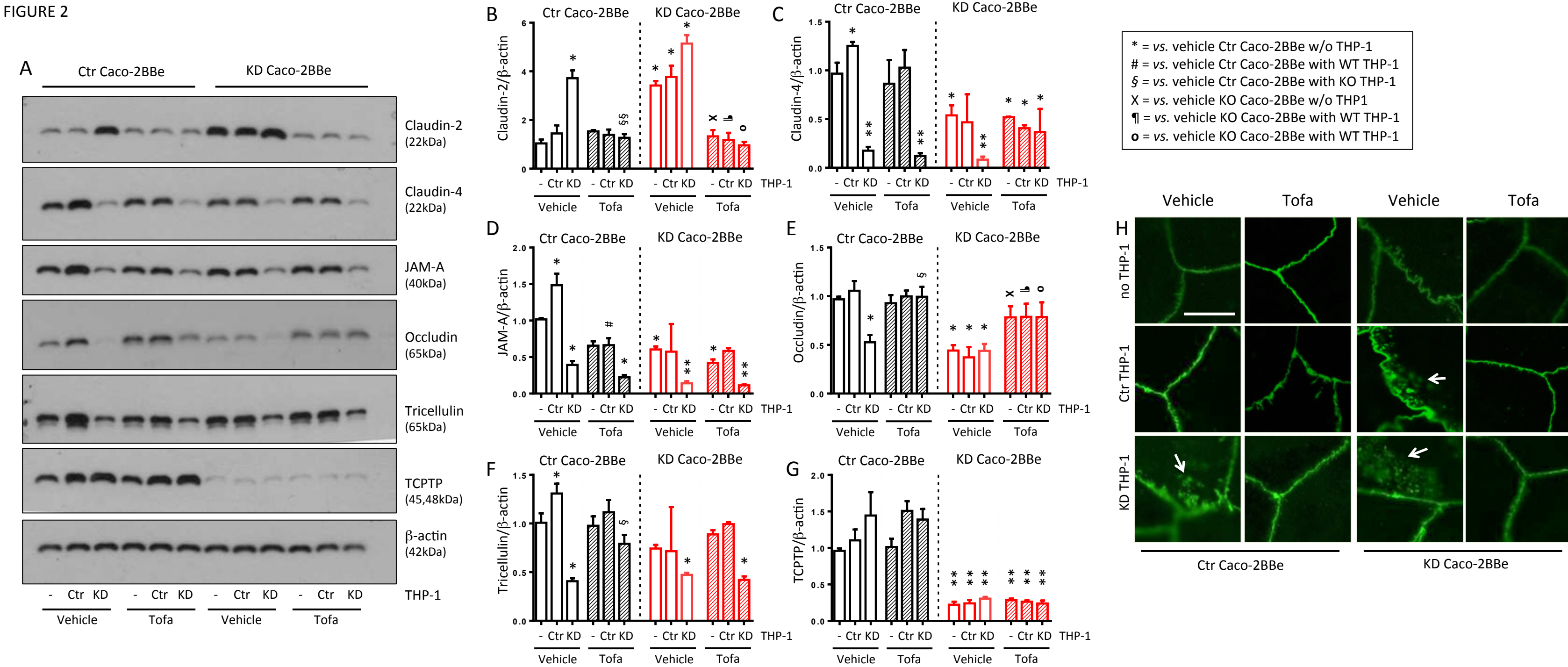


FIGURE 3

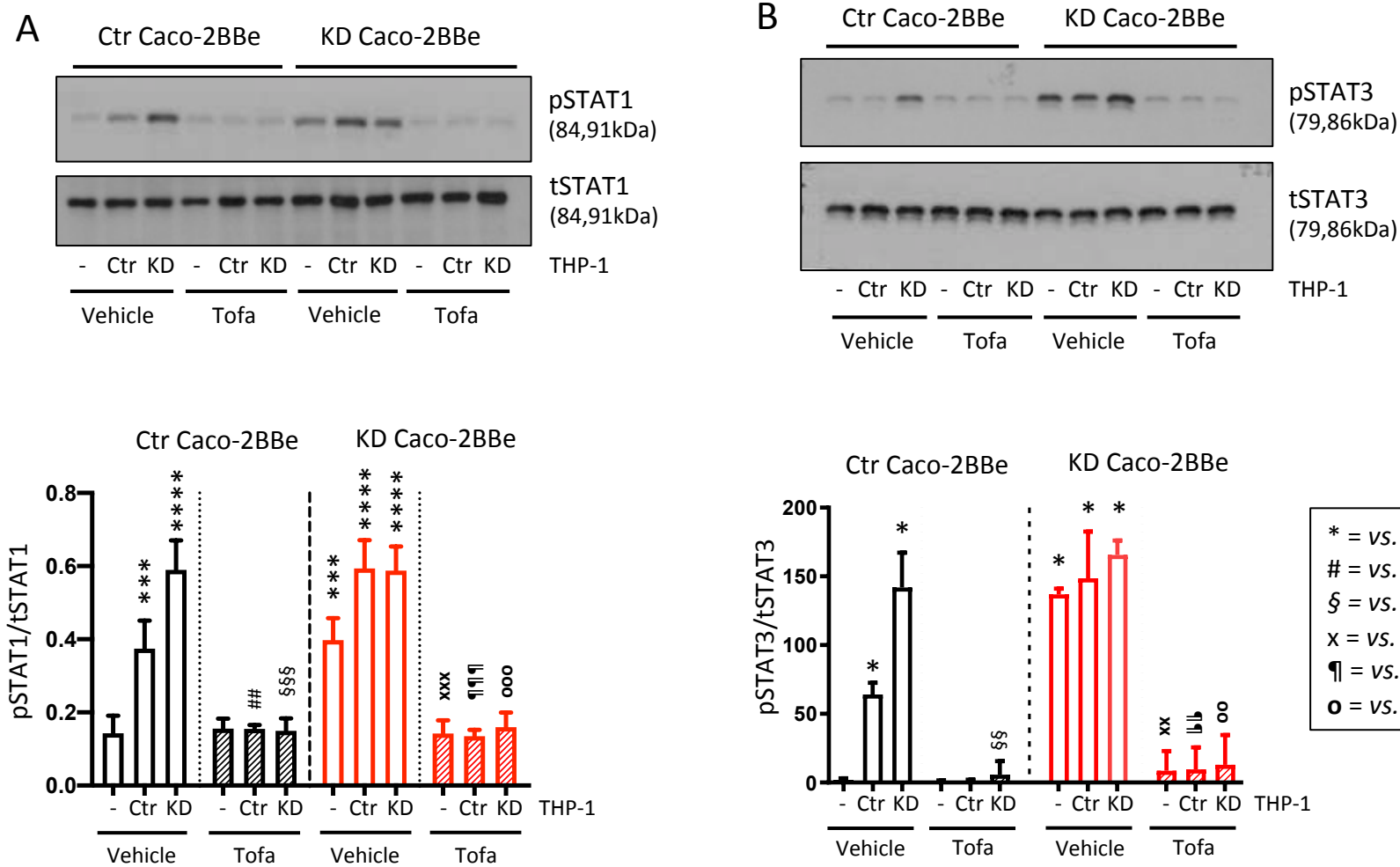


FIGURE 4

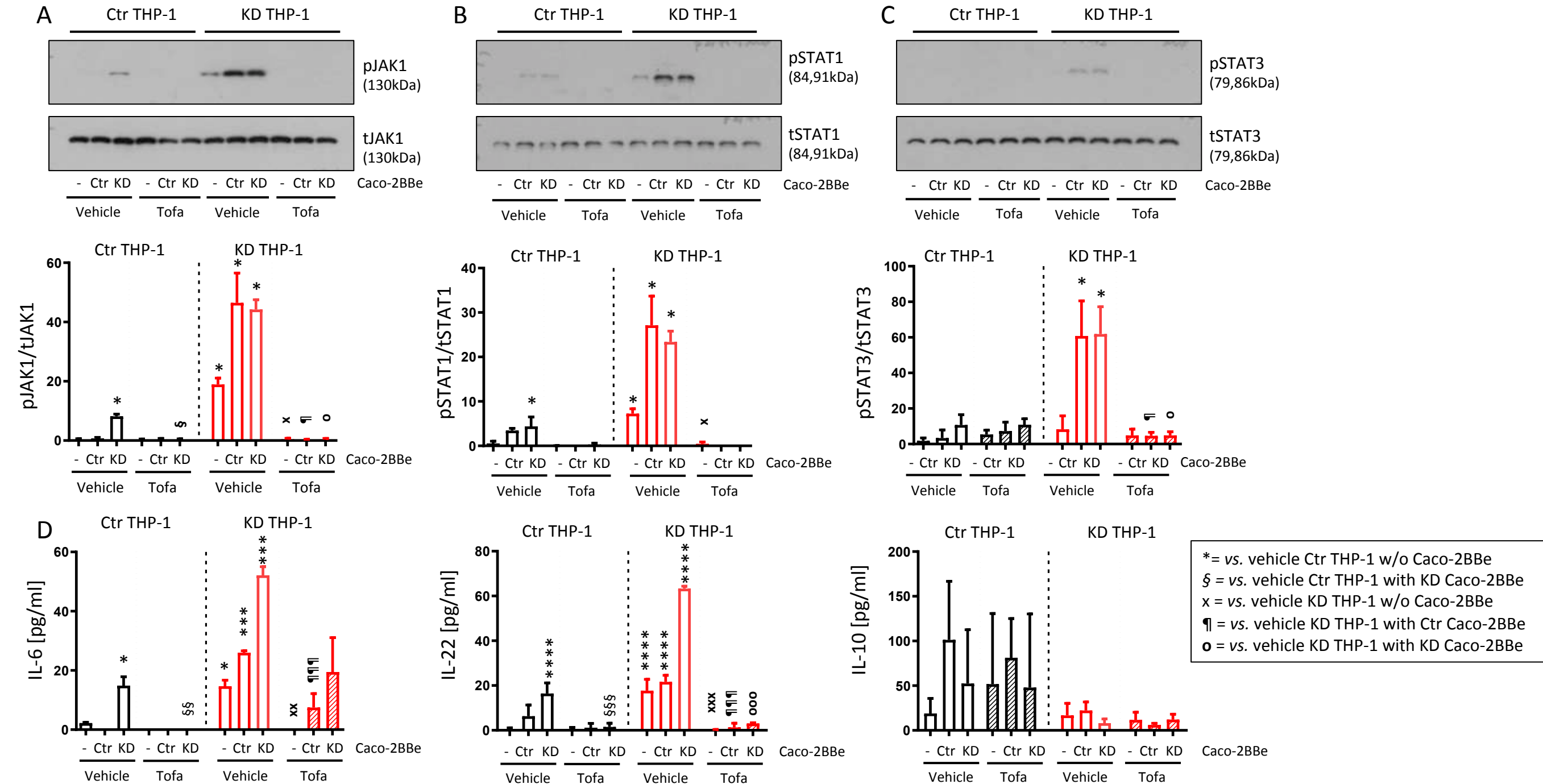


FIGURE 5

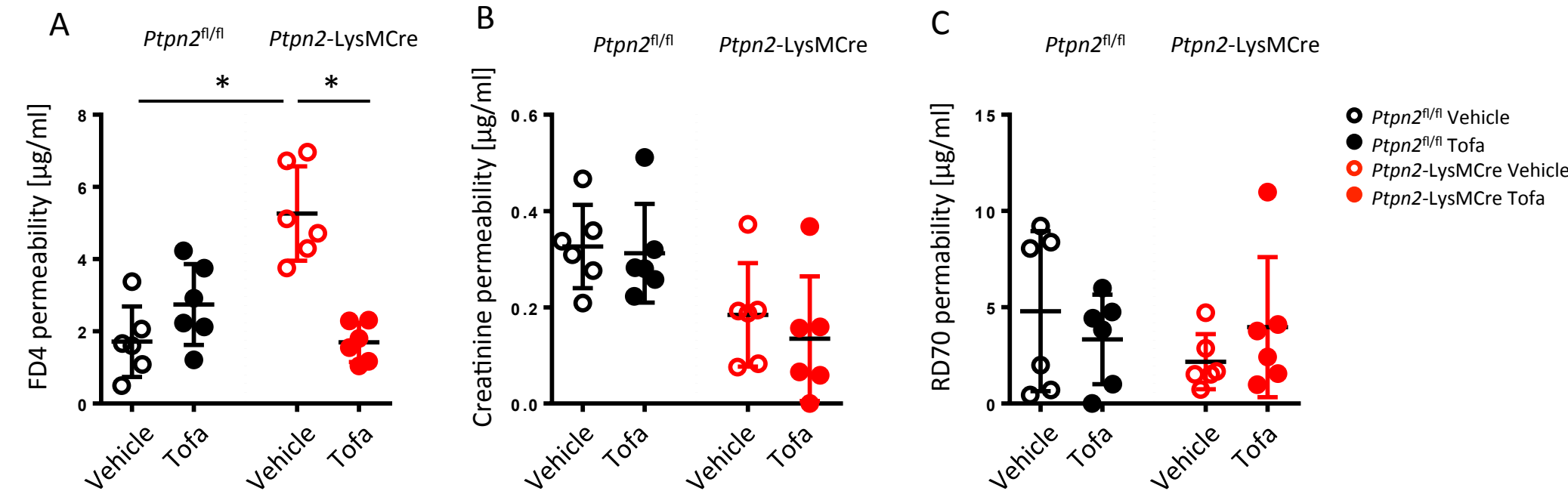


FIGURE 6

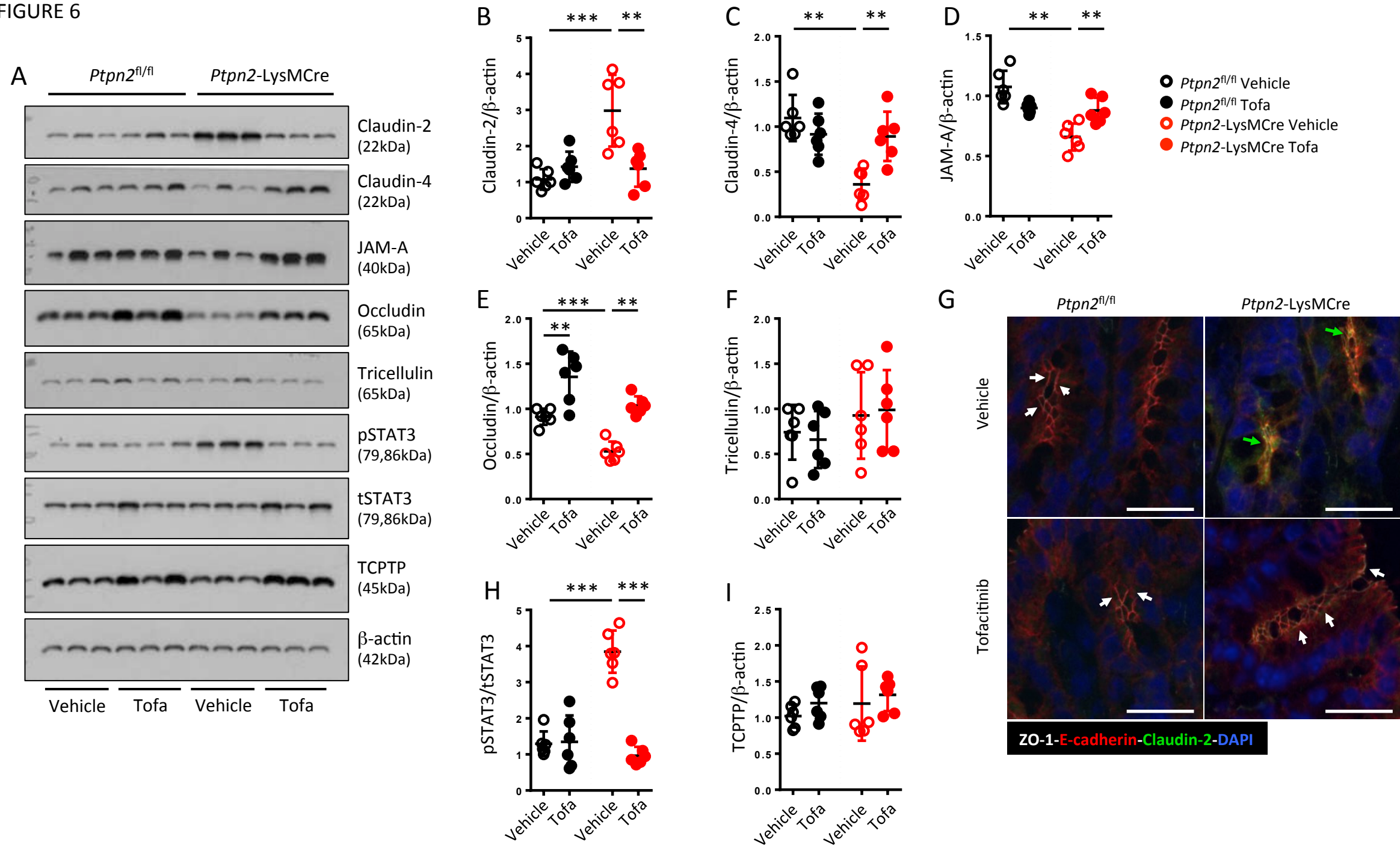
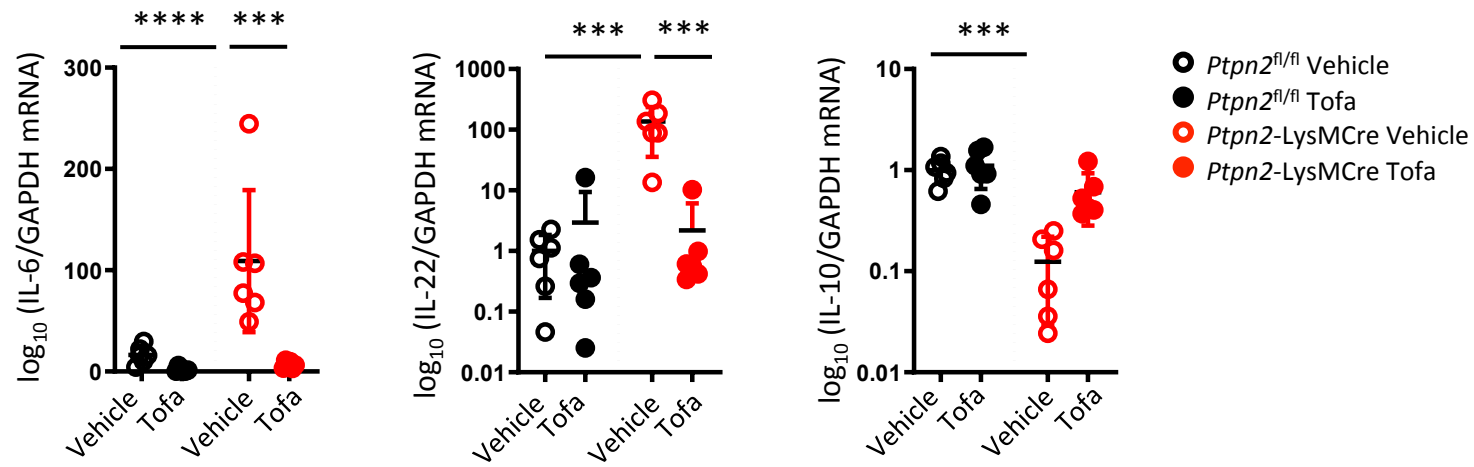
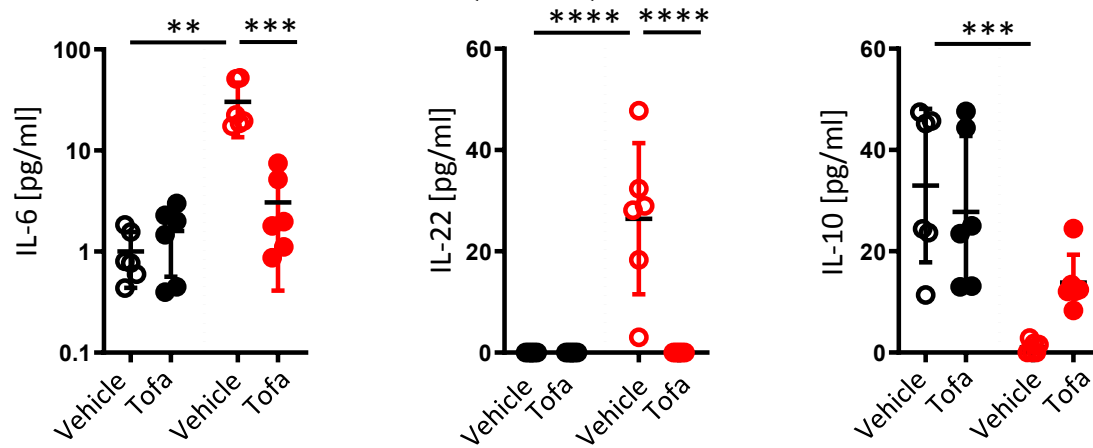


FIGURE 7

A



B



C

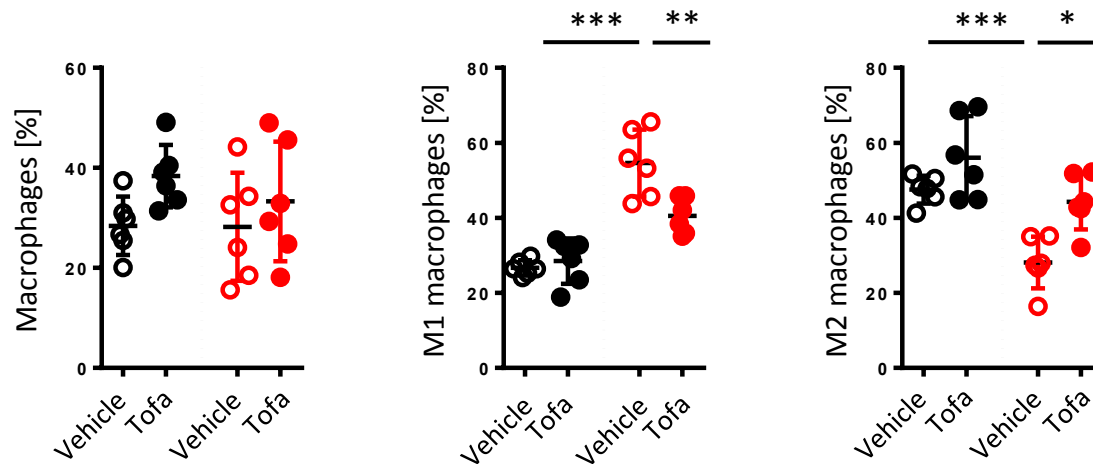
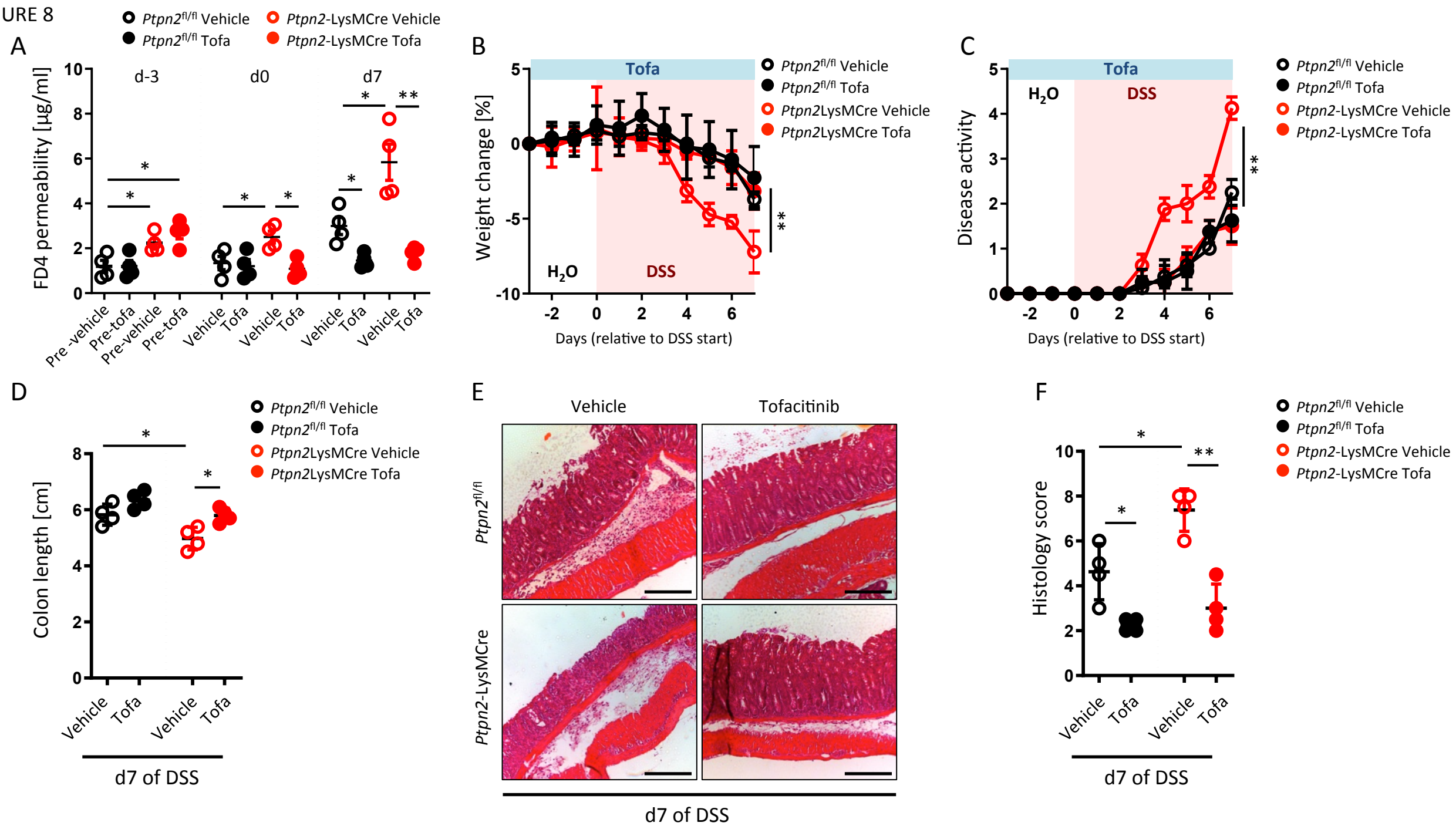
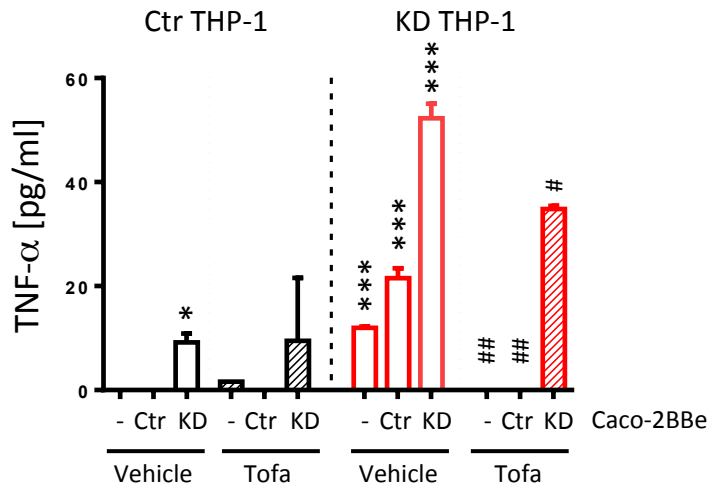
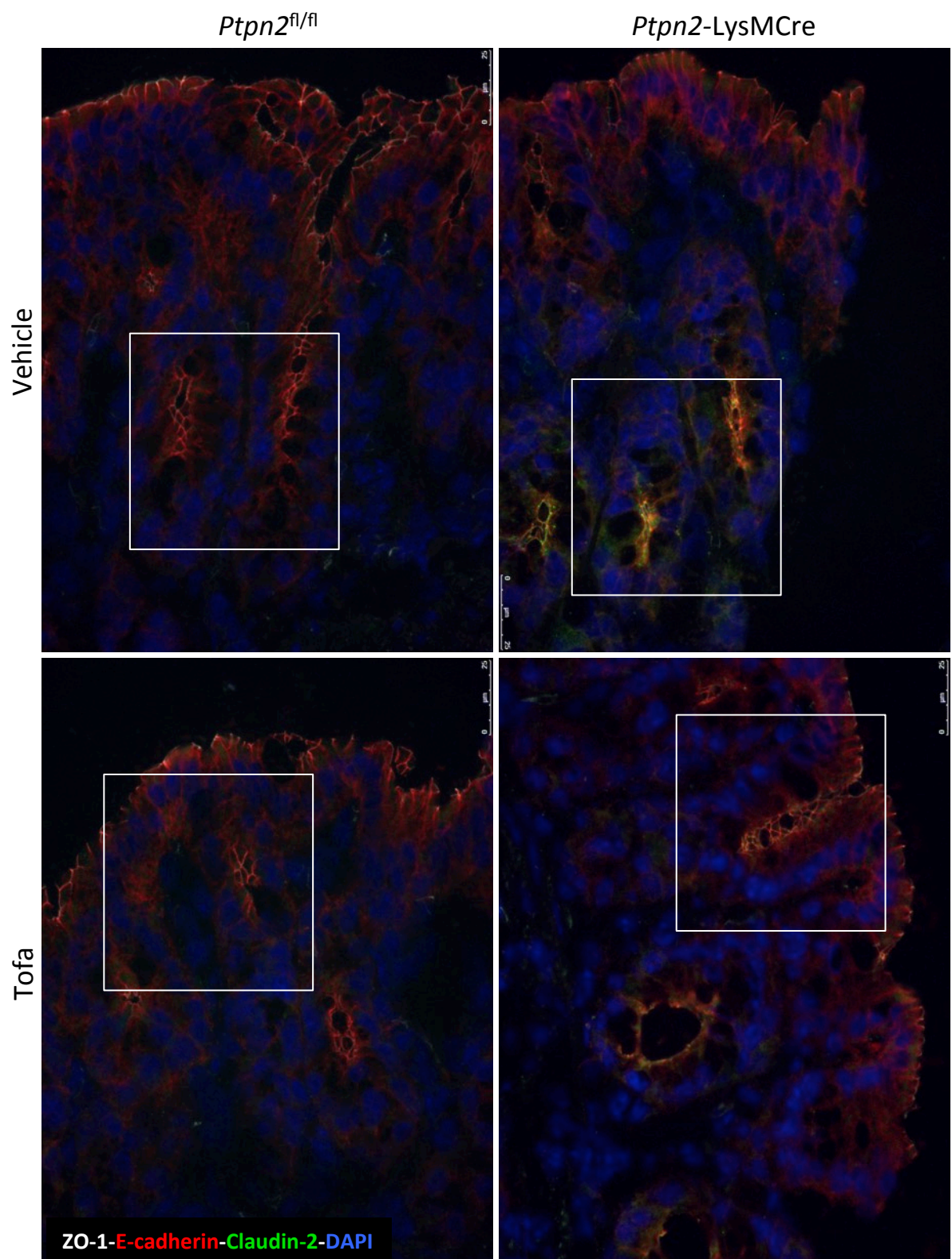


FIGURE 8



SUPP. FIGURE 1





SUPP. FIGURE 3

